Prevailing climatic trends and runoff response from Hindukush-Karakoram-Himalaya, upper Indus basin

Shabeh ul Hasson[1,2], Jürgen Böhner[1], Valerio Lucarini[3,4,1]

[1] CEN, Centre for Earth System Research and Sustainability, University of Hamburg, Hamburg, Germany

[2] Department of Space Sciences, Institute of Space Technology, Islamabad, Pakistan

[3] Department of Mathematics and Statistics, University of Reading, Reading, UK

[4] Walker Institute for Climate System Research, University of Reading, Reading, UK

Correspondence to: S. Hasson (shabeh.hasson@uni-hamburg.de)

Abstract

Largely depending on the meltwater from the Hindukush-Karakoram-Himalaya, withdrawals from the upper Indus basin (UIB) contribute half of the surface water availability in Pakistan, indispensable for agricultural production systems, industrial and domestic use and hydropower generation. Despite such importance, a comprehensive assessment of prevailing state of relevant climatic variables determining the water availability is largely missing. Against this background, this study assesses the trends in maximum, minimum and mean temperatures, diurnal temperature range and precipitation from 18 stations (1250-4500 masl) for their overlapping period of record (1995-2012), and separately, from six stations of their long-term record (1961-2012). For this, Mann-Kendall test on serially independent time series is applied to detect the existence of a trend while its true slope is estimated using the Sen's slope method. Further, locally identified climatic trends are statistically assessed for their spatial scale significance within ten identified sub-regions of the UIB, and the spatially (field) significant climatic trends are then qualitatively compared with the trends in discharge out of corresponding sub-regions. Over the recent period (1995-2012), we find a well agreed warming and drying of spring season (field significant in March) and a rising early-melt season discharge from most of the sub-regions, likely due to a rapid snowmelt. In stark contrast, most of the sub-regions feature a field significant cooling within the monsoon period (particularly in July and September), which coincides well with the main glacier melt season. Hence, a falling or weakly rising discharge is observed from the corresponding sub-regions during mid-to-late melt season (particularly in July). Such tendencies, being largely consistent with the long-term trends (1961-2012), most likely indicate dominance of the nival

but suppression of the glacial melt regime, altering overall hydrology of the UIB in future. These findings, though constrained by sparse and short observations, largely contribute in understanding the UIB melt runoff dynamics and address the hydroclimatic explanation of the 'Karakoram Anomaly'.

1 Introduction

The hydropower generation has key importance in minimizing the on-going energy crisis in Pakistan and meeting the country's burgeoning future energy demands. For this, seasonal water availability from the upper Indus basin (UIB) that contributes to around half of the annual average surface water availability in Pakistan is indispensable for exploiting 3500 MW of installed hydropower potential at country's largest Tarbela reservoir immediate downstream. Withdrawals from the UIB further contribute to the country's agrarian economy by meeting extensive irrigation water demands. The earliest water supply from the UIB after a long dry period (October to March) is obtained from melting of snow (late-May to late-July), the extent of which largely depends upon the accumulated snow amount and the concurrent temperatures (Fowler and Archer, 2005; Hasson et al., 2014b). Snowmelt runoff is then overlapped by the glacier melt runoff (late-June to late-August) that primarily depends upon the melt season temperatures (Archer, 2003). Snow and glacier melt runoffs, originating from the Hindukush-Karakoram-Himalaya (HKH) Ranges, together constitute around 70-80% of the mean annual water available from the UIB (SIHP, 1997; Immerzeel et al., 2009). Unlike major river basins of the South and Southeast Asia that feature extensive summer monsoonal wet regimes downstream, the lower Indus basin is mostly arid and hyper-arid and much relies upon the meltwater from the UIB (Hasson et al., 2014b).

In view of high sensitivity of the mountainous environments to climate change (MRI, 2015; Hasson et al., 2016d) and the role of meltwater as an important control for the UIB runoff dynamics, it is crucial to assess the prevailing climatic state of the UIB and the subsequent water availability. Several studies have been performed in this regard. For instance, Archer and Fowler (2004) have found a significant increase in winter, summer and annual precipitation over the period 1961-1999. For the same period, Fowler and Archer (2006) have found a significant cooling during summer but warming during winter. Sheikh et al. (2009) have documented significant cooling and wetting of the monsoon (July-September) but warming of the pre-monsoon season (April-May) over the 1951-2000 period. Khattak et al.

(2011) have found winter warming, summer cooling (1967-2005), but no definite pattern for precipitation. It is noteworthy that these findings are based upon at least a decade old data records. Analyzing updated data for the last three decades (1980-2009), Bocchiola and Diolaiuti (2013) have suggested that winter warming and summer cooling are less general than previously thought, and can be clearly assessed only for Gilgit and Bunji stations. They have found mostly insignificant precipitation increase over the Chitral-Hindukush and northwest Karakoram while decrease over the Greater Himalayas. Analyzing temperature record for recent six decades (1952-2009), Río et al. (2013) have also reported dominant warming during March and pre-monsoon season.

The above mentioned studies have analyzed observations from only a sub-set of half dozen manual, valley-bottom, low-altitude UIB stations, being maintained by the Pakistan Meteorological Department (PMD). Contrary to low-altitude stations, observations from high-altitude stations in the South Asia mostly feature opposite sign of climatic changes and extremes, possibly influenced by the local factors (Revadekar et al., 2013). Moreover, the bulk of the UIB stream flow originates from the active hydrologic zone (2500-5500 masl), when thawing temperatures migrate over and above 2500 masl (SIHP, 1997). Given such a large altitudinal dependency of the climatic signals, data from the low-altitude stations, though extending back into the first half of 20^{th} century, are not optimally representative of the hydro-meteorological conditions prevailing over the UIB frozen water resources (SIHP, 1997). Thus, the assessment of climatic trends over the UIB has been much restricted by the limited availability of high-altitude and most representative observations as well as their accessibility, so far.

Above mentioned studies of Archer and Fowler (2004), Fowler and Archer (2006) and Sheikh et al. (2009) have used linear least square method for trend analysis. Such parametric tests though robustly assess the trend relative to non-parametric tests (Zhai et al., 2005), but need the sample data to be normally distributed, which is not always the case for hydro-meteorological observations (Hess et al., 2001). Hence, a widely adopted non-parametric test, such as, Mann Kendall (MK - Mann, 1945; Kendall, 1975) is more pragmatic choice, as employed by Khattak et al. (2011), Río et al. (2013) and Bocchiola and Diolaiuti (2013).

Most of the hydro-climatic time series contain red noise because of the characteristics of natural climate variability, and thus, are not serially independent (Zhang et al., 2000; Wang et al., 2008). However, MK statistic is highly sensitive to the serial dependence of a time series

(Yue and Wang, 2002; Yue et al., 2002 & 2003). For instance, the variance of MK statistic *S* increases (decreases) with the magnitude of significant positive (negative) auto-correlation of a time series, which leads to an overestimation (underestimation) of the trend detection probability (Douglas et al., 2000; Wu et al., 2008; Rivard and Vigneault, 2009). To eliminate such affect, von Storch (1995) and Kulkarni and von Storch (1995) proposed a pre-whitening procedure that removes the lag-1 auto-correlation prior to applying the MK test, as employed by Río et al. (2013) amid the above cited studies. However, such procedure is particularly inefficient when a time series either features a trend or is serially dependent negatively (Rivard and Vigneault, 2009). In fact, presence of a trend can lead to false detection of significant positive (negative) auto-correlation in a time series (Rivard and Vigneault, 2009), removing which through a pre-whitening may remove (inflate) the portion of a trend, leading to the underestimation (overestimation) of trend detection probability and trend magnitude (Yue and Wang, 2002; Yue et al., 2003). To avoid this, Yue et al. (2002) proposed a trend free pre-whitening (TFPW) in which the trend component of a time series is separated prior to pre-whitening and then blended back to the resultant time series, as adopted by Khattak et al. (2011). However, prior estimation of the trend may also be influenced by the presence of serial correlation in a time series in a similar way the presence of trend contaminates the estimates of auto-correlation (Zhang et al., 2000). It is, therefore, desirable to estimate the most accurate magnitudes of both, trend and auto-correlation, in order to avoid the influence of one on the other.

The UIB observes contrasting hydro-meteo-cryospheric regimes mainly because of the complex HKH terrain and sophisticated interaction of prevailing regional circulations (Hasson et al., 2014a and 2016a). The sparse meteorological network in such difficult area neither covers fully its vertical nor its horizontal extent - it may also be highly influenced by complex terrain features and variability of meteorological events. Under such scenario, tendencies ascertained from the observations at local sites further need to be assessed for their field significance. The field significance indicates whether the stations within a particular region collectively exhibit a significant trend or not, irrespective of the significance of individual trends (Vogel and Kroll, 1989; Lacombe and McCarteny, 2014). This yields a dominant signal of change and much clear understanding of what impacts the observed conflicting climate change will have on the overall hydrology of the UIB and of its sub-regions. However, alike sequentially dependent local time series, spatial-/cross-correlation amid the station network of a region, possibly present due to the influence of a common

129 climatic phenomenon and/or of similar physio-geographical features (Yue and Wang, 2002),
130 anomalously increases the probability of detecting the field significant trends (Yue et al.,
131 2003; Lacombe and McCarteny, 2014). Therefore, the effect of cross correlation amid the
132 station network needs to be eliminated while testing the field significance (Douglas et al.,
133 2000; Yue and Wang, 2002; Yue et al., 2003). Further, statistically identified field significant
134 climatic trends should be verified against the physical evidence.

135 In this study, we present a first comprehensive and systematic hydroclimatic trend analysis
136 for the UIB based on ten stream flow, six low-altitude manual and 12 high-altitude automatic
137 weather stations. We apply the MK trend test over serially independent hydroclimatic time
138 series for ensuring the existence of a trend while its true slope is estimated by the Sen's slope
139 method. The monthly to annual scale individual trends are further assessed for their field
140 significance within the ten identified sub-regions of the UIB, and in order to furnish the
141 physical attribution to statistically identified regional signal of change, the field significant
142 trends are in turn compared qualitatively with the trends in discharge out of the corresponding
143 regions.

144

145 **2 Upper Indus basin**

146 Spanning over the geographical range of 31-37^{o}E and 72-82^{o}N, the basin extends from the
147 western Tibetan Plateau in the east to the eastern Hindu Kush Range in the west, hosting the
148 Karakoram Range in the north and the western Himalayan massif (Greater Himalaya) in the
149 south (Fig. 1). Around 46 % of the UIB falls within the political boundary of Pakistan,
150 containing around 60% of the permanent cryospheric extent. Based on the Randolph Glacier
151 Inventory version 5.0 (Arendt et al., 2015), around 12% of the UIB area (19,370 km^2) is
152 under the glacier cover. The snow cover varies from 3 to 67% of the basin area (Hasson et al.,
153 2014b).

154 The hydrology of the UIB is dominated by the precipitation regime associated with the year-
155 round mid-latitude western disturbances that intermittently transport moisture mainly during
156 winter and spring and mostly in the solid form (Wake, 1989; Ali et al., 2009; Hewitt, 2011;
157 Hasson et al., 2016a & 2016b). Such moisture contribution is anomalously higher during the
158 positive phase of the north Atlantic oscillation (NAO), when the southern flank of the
159 western disturbances intensifies over Iran and Afghanistan because of heat low there, causing

additional moisture input from the Arabian Sea (Syed et al., 2006). The basin further receives moisture from the summer monsoonal offshoots, which crossing the main barrier of the Greater Himalayas (Wake, 1989; Ali et al., 2009), precipitate over higher (lower) altitudes in solid (liquid) form (Archer and Fowler, 2004). Such occasional incursions of the monsoonal system and the dominating westerly disturbances -- further controlled by the complex HKH terrain -- define the contrasting hydroclimatic regimes within the UIB.

Mean annual precipitation within the basin ranges from less than 150 mm at Gilgit station to around 700 mm at Naltar station. However, the glaciological studies suggest substantially large amounts of snow accumulations that account for 1200-1800 mm (Winiger et al., 2005) in the Bagrot valley and above 1000 mm over the Batura Glacier (Batura Investigation Group, 1979) within the western Karakoram. Within the central karakoram, such amounts account for more than 1000 mm, and at few sites, above 2000 mm over the Biafo and Hispar glaciers (Wake, 1987).

The Indus River and its tributaries are gauged at ten key locations within the UIB, dividing it into Astore, Gilgit, Hunza, Shigar and Shyok sub-basins that feature distinct hydrological regimes (snow- and glacier-fed). Archer (2003) and Mukhopadhyay and Khan (2015) have identified snow-fed (glacier-fed) sub-basins based on their: 1) smaller (larger) glacier cover; 2) strong runoff correlation with previous winter precipitation (concurrent temperatures) from low-altitude stations, and; 3) hydrograph separation. Their findings suggest that Astore and Gilgit are mainly snow-fed while Hunza, Shigar and Shyok are mainly glacier-fed sub-basins. The strong influence of climatic variables on the generated melt runoff suggests high vulnerability of spatio-temporal water availability to climatic changes. This is why the UIB discharge features high variability – the maximum mean annual discharge is around an order of magnitude higher than its minimum mean annual discharge, in extreme cases. Mean annual UIB discharge is around 2400 m^3s^{-1}, which contributing around 45% of the total surface water availability in Pakistan, mainly confines to the melt season (April-September). For the rest of year, melting temperatures remain mostly below the active hydrologic elevation range, resulting in minute melt runoff (Archer, 2004). The characteristics of the UIB and its sub-basins are summarized in Table 1.

3 Data

3.1 Meteorological data

The network of meteorological stations within the UIB is very sparse and mainly limited to within the Pakistan's political boundary, where 20 meteorological stations are being operated by three different organizations. The PMD operates six manual valley-bottom (1200-2200 masl) stations that provide the only long-term record since the first half of 20th century, however, the data before 1960 are scarce and feature large data gaps (Sheikh et al., 2009). EvK2-CNR maintains two high-altitude stations within the central Karakoram, which provide data only since 2005. The third meteorological network being maintained by the Snow and Ice Hydrology Project (SIHP) of the Water and Power Development Authority (WAPDA), Pakistan consists of twelve high-altitude (1479-4440 masl) automated weather stations, called Data Collection Platforms (DCPs), which provide observations since 1994. Contrary to PMD and EvK2-CNR precipitation gauges, DCPs measure snow in mm water equivalent as solid moisture is the main source of melt dominated hydrology of the UIB (Hasson et al., 2014b). Moreover, extending to the Karakoram Range that hosts most of the Indus basin ice reserves (Fig. 1) and covering most of the active hydrologic zone of the UIB (2500-5500) -- unlike PMD stations -- DCPs are well representative of the hydro-meteorological conditions prevailing over the UIB cryosphere, so far. We have collected the daily data of maximum and minimum temperatures (Tx and Tn, respectively) and precipitation from 12 DCPs for the period 1995-2012 and from six PMD stations for the period 1961-2012 (Table 2).

3.2 Discharge data

The daily discharge data of all ten hydrometric stations within the UIB have been collected from the Surface Water Hydrology Project of WAPDA, Pakistan for their full length of available record up to 2012 (Table 3). Among the installed hydrometric stations, Shigar gauge has not been operational since 2001. It is to mention that discharge observations from the central and eastern UIB are hardly influenced by the anthropogenic perturbations. Though the western UIB is relatively populous and the stream flow is used for the solo-seasoned crops and domestic use, the overall water diversion for such use is negligible (Khattak et al., 2011).

4 Methods

We have checked the internal consistency of the data by closely following Klein Tank et al. (2009) such as the situations of below zero precipitation and when maximum temperature was lower than minimum temperature, which found in few were corrected. Then, we have performed homogeneity tests using a standardized toolkit RH-TestV3 (Wang and Feng, 2009) that uses a penalized maximal F-test (Wang et al., 2008) to identify any number of change points in a time series. As no station has yet been reported homogenous at monthly time scale for all variables, only relative homogeneity test was performed by adopting the most conservative threshold level of 99% for the statistical significance. Except Skardu, PMD stations mostly feature one inhomogeneity in only Tn, which over the 1995-2012 period is valid only for Gilgit and Gupis stations (Table 2). The DCP data were found of high quality and homogenous. Only Naltar station has experienced inhomogeneity in Tn during September 2010, which was most probably caused by heavy precipitation event resulted in a mega flood in Pakistan (Houze et al., 2011; Ahmad et al., 2012) followed by similar events in 2011 and 2012. Since history files were not available, it was not sure that any statistically found inhomogeneity only in Tn is real. Thus, we did not apply corrections to inhomogeneous time series and caution the careful interpretation of results based on them.

4.1 Hydroclimatic trend analysis

We have analyzed trends in minimum, maximum and mean temperatures (Tn, Tx and Tavg, respectively), diurnal temperature range (DTR = Tx - Tn), precipitation and discharge on monthly to annual time scales. For this, the MK test (Mann, 1945; Kendall, 1975) is applied to assess the existence of a trend while the Theil-Sen (TS - Theil, 1950; Sen, 1968) slope method is applied to estimate its true slope. The MK is a ranked based method that tests the existence of a trend irrespective of the type of sample data distribution and whether such trend is linear or not (Wu et al., 2008; Tabari and Talaee, 2011). MK is also insensitive to the data outliers and missing values (Bocchiola and Diolaiuti, 2013) and less sensitive to the breaks caused by inhomogeneous time series (Jaagus, 2006). For comparison between low- and high-altitude stations, we have mainly analyzed their overlapping period of record (1995-2012) but additionally the full period of record (1961-2012) for the low-altitude stations.

4.2 Trend-perceptive pre-whitening

The used approach of Zhang et al (2000) assumes that the trend can be approximated as linear (Eqn. 1) and the noise, γ_t, can be represented as pth order auto-regressive process, AR(p) of the signal itself, plus the white noise, ε_t. Since the partial auto-correlations for lags larger

than one are generally found insignificant (Zhang et al., 2000; Wang and Swail, 2001), considering only lag-1 auto-regressive processes, *r*, transforms Eqn. 1 into Eqn. 2:

$$Y_t = a + \beta t + \gamma_t \quad (1)$$

$$Y_t = a + \beta t + rY_{t-1} + \varepsilon_t \quad (2)$$

Then the most accurate magnitudes of lag-1 auto-correlation and trend are iteratively found using the following steps:

1. In first iteration, lag-1 autocorrelation, r_1 is computed on the original time series, Y_t
2. Using r_1 as $(Y_t - r.Y_{t-1})/(1-r)$, intermediate time series, $\acute{Y}_t$, is obtained and its trend, β_1 is computed using TS and MK methods
3. Original time series, Y_t is detrended using $\beta_1$as ($\widehat{Y}_t = Y_t - \beta_1 t$)
4. In second iteration, lag-1 autocorrelation, r_2 is estimated on detrended time series, $\widehat{Y}_t$
5. Original time series, Y_t is again pre-whitened using r_2 and $\acute{Y}_t$ is obtained
6. Trend, β_2 is then computed on $\acute{Y}_t$ and Y_t is detrended again, yielding $\widehat{Y}_t$

The steps have to be reiterated until r is no longer significantly different from zero or the absolute difference between the estimates of r, β obtained from two consecutive iterations becomes less than one percent. If any of the condition is met, let's suppose at the iteration *n*, the estimates from previous iteration (i.e. $r = r_{n-1}, \beta = \beta_{n-1}$) are used in Eqn. 3 to obtain a pre-whitened time series, Y_t^w which features the same trend as of the original time series, Y_t (Zhang et al., 2000; Wang and Swail, 2001).

$$Y_t^w = \frac{(Y_t - r.Y_{t-1})}{(1-r)} = \hat{a} + \beta t + \epsilon_t \text{ , where } \hat{a} = a + \frac{r.\beta}{(1-r)} \text{ , and } \epsilon_t = \frac{\varepsilon_t}{(1-r)} \quad (3)$$

4.3 Field significance and physical attribution

Field significance implies whether two or more stations within a particular region collectively exhibit a significant trend, irrespective of the significance of their individual trends (Vogel and Kroll, 1989; Lacombe and McCarteny, 2014). The field significance of climatic variables has been assessed for the ten sub-regions of the UIB identified based on: 1) distinct hydrological regimes; 2) mountain divides, and; 3) installed hydrometric stations. Further, statistically identified field significant climatic trends were qualitatively compared to the physically-based evidence of trend in discharge out of corresponding region, in order to establish more confidence. As outlet discharges describe the integrated signal of hydrologic change within the basin, testing their field significance was not required.

283 The Shigar has continuous discharge only till 1998 where its post-1998 discharge needs to be
284 derived. For this, Mukhopadhyay and Khan (2014) have estimated the pre-1998 monthly
285 correlation coefficients between Shigar and its immediate downstream Kachura gauge and
286 applied these coefficients to the post-1998 Kachura discharge. However, such approach
287 yields merely a constant fraction of the Kachura discharge as the applied coefficients are less
288 likely to remain invariant after 1998, in view of the large drainage area of Indus at Kachura
289 (113,000 km^2) and the hydroclimatic changes expected upstream Shigar gauge. Here, instead
290 of estimating the post-1998 discharge at the Shigar gauge, we have derived the discharge for
291 the Shigar-region that comprises the Shigar sub-basin itself plus the adjacent region shown in
292 blank in Figure 2. This was achieved by subtracting the discharge rates of all gauges
293 upstream Shigar gauge from its immediate downstream gauge of Kachura, for each time step
294 of every time scale analyzed. The procedure assumes that the gauges far from each other have
295 negligible routing time delay at the analyzed mean monthly time scale and that such
296 approximation does not further influence the ascertained trends. Similar approach was
297 adopted to derive discharges out of ungauged identified sub-regions (Table 1).

298 We have considered the combined drainage area of Shyok and Shigar-region as UIB-Central
299 and the drainage area of Indus at Kharmong as UIB-East (Fig. 2). The rest of the UIB is
300 named as UIB-West (Fig. 2), which is further divided into upper and lower parts due to their
301 distinct hydrological regimes. Here, these regimes are identified based on the timings of
302 maximum runoff production from the median hydrographs of each hydrometric station.
303 According to such division, UIB-West-lower and Gilgit are mainly the snow-fed while Hunza
304 is mainly the glacier-fed (Fig. 3). Since the most of Gilgit basin area lies at the Hindukush
305 massifs, we call it Hindukush region. The combined area of UIB-West-lower and UIB-east
306 mainly contains the northward slopes of the Greater Himalaya, so we call it Himalaya.
307 Similarly, drainage areas of Hunza, Shyok and Shigar-region are named as western, eastern
308 and central Karakoram, respectively, that collectively constitute the Karakoram region.

309 For assessing the field significance, we have used the method of Yue et al. (2003), which
310 preserves the cross correlation amid the stations network but eliminates its effect on testing
311 the filed significance through resampling the original network using bootstrapping approach
312 (Efron, 1979), in our case 1000 times. The method considers the counts of significant trends
313 as the representative variables. Unlike MK statistics, *S* or its regional average (Douglas et al.,
314 2000; Yue and Wang, 2002) 'counts' variable favourably provides a measure of dominant

315 field significant trend when both positive and negative significant trends are present. The
316 method counts both the number of local significant positive trends and the number of
317 significant negative trends separately for each of 1000 resampled networks using Eqn. 10:

318 $$C_f = \sum_{i=1}^{n} C_i \quad (10)$$

319 Where n denotes total number of stations within a region and C_i denotes a count for
320 statistically significant trend (at 90% level) at station, i. Then, the empirical cumulative
321 distributions C_f were obtained for both counts of significant positive trends and counts of
322 significant negative trends, by ranking their 1000 values in an ascending order using Eqn.11:

323 $$P\left(C_f \leq C_f^r\right) = \frac{r}{N+1} \quad (11)$$

324 Where r is the rank of C_f^r and N denotes the total number of resampled network datasets. We
325 have estimated the probability of counts of significant positive (negative) trends in actual
326 network by comparing the number with C_f for counts of significant positive (negative) trends
327 obtained from resampled networks (Eqn. 12).

328 $$P_{obs} = P\left(C_{f,obs} \leq C_f^r\right),\ where\ P_f = \begin{cases} P_{obs} & for\ P_{obs} \leq 0.5 \\ 1 - P_{obs} & for\ P_{obs} > 0.5 \end{cases} \quad (12)$$

329 If $P_f \leq 0.1$ is satisfied the trend for a region is considered to be field significant at 90% level.

330 We have intentionally avoided the interpolation of data and results in view of the limitations
331 of interpolation techniques in HKH complex terrain. Large offset of glaciological estimates
332 from the station-based precipitation amounts (Hasson et al., 2014b) further suggests that the
333 hydroclimatic patterns are highly variable in space and that the interpolation will add to
334 uncertainty, resulting in misleading conclusions.

335

336 **5 Results**

337 Results for the 1995-2012 period are presented in Tables 4-5 (and for select months, in Fig.
338 4) while Table 6 presents results for the 1961-2012 period. Field significant climatic and
339 discharge trends of corresponding regions are given in Table 7.

340 **5.1 Hydroclimatic trends**

341 **Mean maximum temperature**

During months of March, May and November, most of the stations suggest mostly insignificant warming, which in terms of magnitude and significance, dominates during March and at the low-altitude stations (Table. 4 and Fig. 4). In contrast, during the monsoon (July-October) and in February, most of the stations suggest cooling, which being similar in magnitude amid low- and high-altitude stations, dominates in September followed by in July in terms of both magnitude and statistical significance (at 12 and 5 stations, respectively). Moreover, the observed cooling dominates the observed warming. For the rest of the months, there is a mixed response of mostly insignificant cooling and warming trends. On a typical seasonal scale, there is a high agreement on spring warming, summer and autumn cooling but a mixed response for winter and annual timescales.

While looking only at long-term trends (Table 6), we note that summer cooling (warming outside summer) in Tx is less (more) prominent and insignificant (significant) at relatively high-altitude stations, such as, Skardu, Gupis, Gilgit and Astore. When compared with trends over the shorter period of 1995-2012, strong long-term warming is restricted to spring months mainly during March and May. Similarly, long-term summer cooling period of June-September has been shifted to July-October.

Mean minimum temperature

The dominant feature of Tn is November-June insignificant warming, which contrary to warming in Tx, is observed higher at the high-altitude stations than at the low-altitude stations (Table 4 and Fig. 4). In contrast to August cooling in Tx, stations suggest a minute and mostly insignificant warming in Tn. In contrast to mostly insignificant warming, we have also found cooling in Tn during months of July, September and October, which though similar in magnitude amid low- and high-altitude stations, dominates in September followed by in July (significant at 8 and 4 stations, respectively) as well as over the general Tn warming, alike Tx.

On a typical seasonal scale, our results suggest warming during winter and spring, cooling during summer and a mixed response for the autumn season. The observed warming dominates during spring. It is noted that a clear signal of significant September cooling has been lost when trend has been assessed on seasonally averaged observations for autumn (combining October and November months). This is further notable from the annual time scale, on which warming trends (significant at 5 stations) dominate instead of cooling trends.

While looking only at low-altitude stations (Table 6), we note that long-term non-summer warming (summer cooling) in Tn is less (more) prominent and insignificant (significant) at stations of relatively high-altitude, such as, Skardu, Gupis, Gilgit and Astore. The long-term warming of winter months is mostly absent over the period 1995-2012.

Mean temperature

Trends in Tavg are dominated by trends in Tx during the July-October period and by Tn during the rest of year (Tables 4-5). Similar to Tx, Tavg features dominant cooling in September, followed by in July and October (significant at 10, 4 and 1 stations, respectively). In contrast, warming dominates in March, which is significant at five stations. Additionally, insignificant warming tendencies observed in May and November are well agreed amid most of the stations (Table 5, Fig. 4). On a typical seasonal timescale, the magnitude of winter and spring warming is observed higher than that of summer and autumn cooling, leading to dominant though mostly insignificant warming on annual timescale. The long-term trends generally suggest cooling tendencies for the Jun-October period but warming for the rest of year. On a seasonal timescale, low-altitude stations unanimously agree on long-term and mostly significant summer cooling. For the annual timescale, a mixed response is found.

Diurnal temperature range

DTR is generally found narrowing throughout the year except for March and May, where particularly low-altitude stations suggest its widening either owing to higher Tx warming or higher Tn cooling (Table 4, Fig. 4). With high inter-station agreement, narrowing of DTR is particularly significant in September followed by in February and associated with higher cooling in Tx than in Tn, higher warming in Tn than in Tx or cooling in Tx but warming in Tn. Narrowing DTR is more prominent at high-altitude stations and during winter, autumn and annual timescales. We note that the long-term (1961-2012) year-round DTR widening observed at low-altitude stations (Table 6) is mainly restricted to March and May, and to some extent, October and December over the period 1995-2012 (Table 4).

Total precipitation

Generally, March-June months are featuring decreasing precipitation trends, which are significant at 7, 5, 2 and 4 stations, respectively (Table 5 and Fig. 4). Similarly, significant drying is observed during August and October at three stations while Rattu station suggests year-round drying except in January and February. High inter-stations agreement is observed

for rising September and winter precipitation, which is higher at high-altitude than at low-altitude stations. Most of the stations within the UIB-West-upper (monsoon dominated region) exhibit an increasing trend. Six stations (Shendure, Yasin, Ziarat, Rattu, Shigar and Chillas) feature significant precipitation increase in either all or at least one of the monsoon months. Such precise response of monthly wetting and drying has been averaged out on seasonal to annual timescales, suggesting increase (decrease) for autumn and winter (spring and summer) but a mixed response for annual precipitation.

Comparison of long-term trends at low-altitude stations (1961-2012) with their trends over recent period (1995-2012) suggests that the long-term spring drying particularly of March and April months and wetting of September (the last monsoonal) month has recently been intensified while the long-term increasing summer precipitation has been changed to decreasing (See Tables 5 and 6).

Discharge

From Figure 3, we clearly show that snow and glacier melt regimes of the UIB can be differentiated from the maximum runoff production timing based on the median hydrographs of available gauges. Figure 3 suggests that Indus at Kharmong (UIB-East), Gilgit at Gilgit (Hindukush) and Astore at Doyian basins that generally feature their peak runoffs in June/July are primarily snow fed while the rest that feature peak runoff in August are mainly glacier fed.

Over the 1995-2012 period, discharge change pattern seems to be more consistent with tendencies in temperature than in precipitation record. Most of the hydrometric stations feature increasing discharge during October-June (dominant during May-June) but decreasing discharge during July, which is significant for five high-altitude/latitude glacier-fed sub-regions (Karakoram, Shigar, Shyok, UIB-Central and Indus at Kachura), mainly owing to drop in July temperatures (Table 5). There is a mixed response for August and September months, however, significant trends suggest an increasing discharge from two regions (Hindukush and UIB-West-lower) in August and from four sub-regions (Hindukush, western-Karakoram, UIB-West-lower and UIB-west) in September.

Despite dominant September cooling, discharge drops mainly during July, suggesting it as month of effective cooling. Discharge of July is also decreasing for the whole UIB though such trend is not significant. During winter, spring and autumn seasons, discharge at most

435 sites feature increasing trend while during summer season and on an annual time scale there
436 is a mixed response.

437 Long-term discharge is generally rising from November to May (Table 6), where such rise is
438 higher in magnitude and mostly significant in May. There is a mixed response for June-
439 October. Consistently on coarser temporal scale, winter discharge is rising while a mixed
440 response is observed for other seasons and on annual timescale. While comparing the long-
441 term trends with those assessed over 1995-2012 period, we note prominent shifts in the sign
442 of trends for the seasonal transitional month of June and within the high flow period of July-
443 September. Such shifts may attribute to recent higher summer cooling accompanied by the
444 enhanced monsoonal precipitation. For instance, long-term July discharge is rising for
445 eastern-, central- and whole Karakoram, UIB-Central, Indus at Kachura, Indus at Partab
446 Bridge and Astore but falling for other sub-regions. In contrast, trends over recent two
447 decades feature opposite signs, except for Astore, UIB-West-upper and its sub-regions.

448 **5.2 Field significance and physical attribution**

449 We present the mean of positive and negative field significant trends from each region (if
450 both exist) in order to present the dominant signal (Table 7). Results show unanimous field
451 significant warming for most of the regions in March followed by in August. Similarly, field
452 significant drying is found in March over all regions, except Karakoram and UIB-Central.
453 Alike local trends, we find field significant cooling over all regions in July, September and
454 October, which on a seasonal timescale, dominates in autumn followed by in summer. Note
455 that most of the climatic trends are not field-significant for the transitional (or pre-
456 monsoonal) period of April-June.

457 We find a general trend of narrowing DTR, which is associated with either warming of Tn
458 against cooling of Tx or relatively lower cooling in Tn than in Tx. Field significant drying of
459 the lower latitudinal generally snow-fed sub-regions (Astore, Himalaya, UIB-West-lower) is
460 also observed particularly during March-September, thus for spring and summer and on
461 annual timescale. On the other hand, wetting (drying) of winter and autumn (spring and
462 summer) is observed for the Hindukush, UIB-West, UIB-West-upper and whole UIB. For the
463 western Karakoram, increasing precipitation is observed only for winter. For the whole
464 Karakoram and UIB-central, field-significant rising precipitation trend is found throughout a
465 year, except for spring where no signal is evident.

Moreover, field significant climatic trends are mostly in qualitative agreement with the trends in discharge from the corresponding regions. Such an agreement is high during summer, particularly for July, and during winter, for March. Few exceptions to such consistency are the sub-regions of Himalaya, UIB-West and UIB-West-lower, for which, in spite of the field significant cooling in July, discharge is still rising. However, the magnitude of rise in July discharge has substantially dropped when compared to previous (June) and following (August) months. Such substantial drop in July discharge increase rate is again consistent with the field significant cooling in July for the UIB-West and UIB-West-lower. Further, besides substantial cooling (warming) in September (March), most prominent decrease in discharge is observed in July while its decrease in May, suggesting them months of effective cooling and warming, respectively. Generally, periods of runoff decrease (in a sequence) span from May to September for the Karakoram, June to September for the UIB-Central, July to August for the western-Karakoram and UIB-West-upper, July to November for the Astore and only over July for the Hindukush and UIB. UIB-West-lower and Himalaya suggest decrease in discharge during months of April and February, respectively.

6 Discussions

6.1 Cooling trends

Observed long-term summer and autumn (or monsoon) cooling is mostly consistent with the earlier reports for the study basin (Fowler and Archer, 2005 and 2006; Khattak et al., 2011; Sheikh et al., 2009), as well as those, for the neighboring regions, such as, Nepal, Himalayas (Sharma et al., 2000; Cook et al., 2003), northwest India (Kumar et al., 1994), Tibetan Plateau (Liu and Chen, 2000), central China (Hu et al., 2003), and central Asia (Briffa et al., 2001).

Over the 1995-2012 period, field significant cooling observed mostly in July, September and October for all UIB sub-regions coincides with the monsoonal onset and retreat months, and most importantly, with the main glacier melt season, thus anticipated to negatively affect the glacier melt runoff. The observed cooling phenomenon is generally attributed to the incursions of the south Asian summer monsoonal system and its precipitation (Cook et al., 2003) into the Karakoram and the UIB-West that presently seems to be accelerated in view of the observed increase in cloud cover, precipitation and number of wet days (Bocchiola and

Diolaiuti, 2013). Since summer precipitation over the UIB is partly received from the westerly disturbances (Wake 1987), the observed cooling may also be attributed to the enhanced influence of the westerly disturbances during summer months, alike during winter and spring (Madhura et al., 2015). Nevertheless, observed increase in cloud cover leads to reduction of incident downward radiations and results in cooling (or less warming) of Tx. Forsythe et al. (2015) have consistently observed the influence of cloud radiative effect on the near surface air temperature over the UIB. The enhanced cloudy conditions most probably are responsible for initial warming in Tn through longwave cloud radiative effect, and when such conditions persist longer in time, Tx and Tn more likely tend to cool. Under the clear sky conditions, cooling in Tx further continues as a result of evaporative cooling of the moisture-surplus surface under precipitation event (Wang et al., 2014) or due to irrigation (Kueppers et al., 2007). Han and Yang (2013) found irrigation expansion over Xinjiang, China as a major cause of observed cooling in Tavg, Tx and Tn during May-September over the period 1959-2006. Further, higher drop in Tn observed over UIB-West-lower during winter may be attributed to intense nighttime cooling of the deforested, thus moisture deficit, bare soil surface, exposed to direct day time solar heating as explained by Yadav et al. (2004). The relevance of such hypotheses for the UIB further needs a detailed investigation of the land-atmosphere processes and feedbacks using high-resolution climate model simulations with explicitly resolved convections, which is beyond the scope of our analysis.

6.2 Warming trends

Long-term warming during November-May is generally found consistent with earlier reports of warming (Fowler and Archer, 2005 and 2006; Sheikh et al., 2009; Khattak et al., 2011; Río et al., 2013) as well as with decreasing snow cover in spring (1967-2012) over the Northern Hemisphere and worldwide (IPCC, 2013) and in winter (2001-2012) over the study region (Hasson et al., 2014b). Consistent with the findings of Sheikh et al. (2009) and Río et al. (2013), warming dominates in spring months where it is field significant in March over almost all identified sub-regions of the UIB. Under the drying spring scenario, less cloudy conditions associated with increasing number of dry days for the westerly precipitation regime (Hasson et al., 2016a & 2016b) together with the snow-albedo feedback can partly explain spring warming. Contrary to long-term warming trends analyzed here or to those previously reported, a field significant cooling is found for winter, which is consistently

observed over the eastern United States, southern Canada and much of the northern Eurasia (Cohen et al., 2012).

6.3 Wetting and drying trends

Field significant rising precipitation for the sub-regions of relatively higher latitudes (Hindukush and UIB-Central, and thus, for the UIB-West-upper, Karakoram and the whole UIB) may be attributed to the enhanced late-monsoonal or westerly precipitation regimes at high-altitude stations. Whereas, shift of the long-term summer (June-August) wetting to drying at the low-altitude stations over the period 1995-2012 indicates a recent transition towards weaker monsoonal influence therein.

The field significant precipitation increase during winter but decrease during spring anticipates certain changes within the westerly precipitation regime. The field significant spring drying (except for Karakoram) is mainly consistent with the weakening and northward shift of the mid-latitude storm track (Bengtsson et al., 2006) and also with increasing number of spring dry days (Hasson et al., 2016a & 2016b). On the other hand, observed winter precipitation increase for relatively high latitudinal sub-regions is more consistent with the observed more frequent incursions of the westerly disturbances therein (Cannon et al., 2015; Madhura et al., 2015). Nevertheless, in view of the enhanced influence of prevailing weather systems and certain changes expected in their seasonality/intermittency under changing climate (Hasson et al., 2016a & 2016b), we speculate significant changes in the timings of the melt water availability from the UIB. Such hypothesis can be tested by assessing changes in the seasonality of observed precipitation and runoff.

6.4 Water availability

The long-term discharge tendencies are consistent with earlier reports from Khattak et al. (2011) for Indus at Kachura, and UIB and from Farhan et al. (2014) for Astore. Similarly, rising and falling discharge trends from Shyok and Hunza sub-basins, respectively, are consistent with Mukhopadhyay et al. (2015). The discharge trends from Shigar-region, though statistically insignificant, are only partially consistent with Mukhopadhyay and Khan (2014), exhibiting agreement for an increasing trend in June and August but a decreasing trend in July and September. Further, prominent shifts of the long-term trends of rising melt-season discharge into falling over the period 1995-2012 for mostly the glacier-fed sub-regions (Indus at Kachura, Indus at Partab Bridge, Eastern-, Central- and whole-Karakoram

559 and UIB-Central) may attribute to higher summer cooling together with certain changes in
560 prevailing precipitation regimes.

561 Over the 1995-2012 period, significant decreasing trend in July discharge is most probably
562 attributed to observed July cooling, which though less prominent than cooling in September,
563 is much effective as it coincides with the main glacier melt season. A drop in July discharge
564 further indicates reduced melt water availability but at the same time positive basin storage,
565 particularly under prevailing wetter conditions. Similarly, rising discharge during May and
566 June most likely is due to the observed warming, which though less prominent than warming
567 in March, is much effective since it coincides with the snowmelt season. This suggests an
568 early melt of snow and subsequent increase in the melt water availability, but concurrently, a
569 lesser amount of snow available for the subsequent melt season. These seasonally distinct
570 changes emphasize on the separate assessments of snow and glacier melt regimes, for which
571 an adequate choice is the hydrological models, which are able to independently simulate
572 snow and glacier melt processes, e.g. University of British Columbia (UBC) watershed
573 model. Based on the UBC model, Hasson et al. (2016c) has recently confirmed our findings
574 that the continuation of prevailing early-melt season warming will yield an increased and
575 early snowmelt runoff, but in stark contrast, mid-to-late melt season cooling will result in a
576 decreased and delayed glacier melt runoff in near future. Such changes in both snow and
577 glacier melt regimes all together can result in a sophisticated alteration of the hydrological
578 regimes of the UIB, and subsequently, the timings of the downstream water availability.

579 Although discharge change pattern seems to be more consistent with the field significant
580 temperature trends, indicating cryospheric melt as a dominating factor in determining the
581 UIB discharge variability, it can also be substantially influenced by changes in the
582 precipitation regimes. For instance, monsoonal offshoots intruding into the study region
583 ironically result in declining river discharge (Archer, 2004). In fact, high albedo of fresh
584 snow reduces the incident energy that results in immediate drop in the melt. The fresh snow
585 also insulates the underlying glacier/ice, slowing down the whole melt process till earlier
586 albedo rates are achieved. Thus, melting of cryosphere and subsequent water availability is
587 also inversely correlated to the number of snowfall events/days during the melt season
588 (Wendler and Weller, 1974; Ohlendorf et al., 1997).

589 In view of the sparse observational network analyzed here, we need to clarify that the
590 observed cooling and warming is only an aspect of the wide spread changes prevailing over

591 the wide-extent UIB basin. This is much relevant for the UIB-Central where we have only
592 one station each from the eastern- and central-Karakoram (UIB-Central) that is not
593 exclusively representative of the hydro-climatic state of corresponding sub-region. Thus, field
594 significant results for the whole Karakoram are mainly dominated by the contribution of
595 relatively large number of stations from the western-Karakoram. Nevertheless, reports of
596 increasing end-of-summer snow covers and falling regional snow line altitudes (Minora et al.,
597 2013; Hasson et al., 2014b; Tahir et al., 2016), increasing or stable glacial extents (Hewitt,
598 2005; Scherler et al., 2011; Bhambri et al., 2013; Minora et al., 2013), and possibly a non-
599 negative glaciers' mass balance within eastern- and central-Karakoram (Gardelle et al., 2013
600 - contrary at shorter period – Kääb et al., 2015), local climate change narratives (Gioli et al.,
601 2013) and overall simulated reduced near-future water availability for the UIB (Hasson et al.,
602 2016c), reinforce our presented findings.

603 We find a common response of hydroclimatic changes from a certain set of months, which
604 are different than those (DJF, MAM, JJA, SON) typically considered for winter, spring,
605 summer and autumn seasons, respectively. This emphasizes on analyzing the hydroclimatic
606 observations on higher temporal resolution to robustly assess the delicate signals of change.

607 It is to mention that the hydro-climatic regime of the UIB is substantially controlled by the
608 interaction of large scale circulation modes and their associated precipitation regimes, which
609 are in turn controlled by the global indices, such as, NAO and ENSO etc. However, time
610 period covered by our presented analysis is not long enough to disintegrate the natural
611 variability signals from the transient climate change. These phenomena need to be better
612 investigated over the longer and spatially complete observational record, thus preferably
613 including the extensive database of validated proxy observations since the challenges of short
614 and sparse robust in-situ observations are most likely to remain invariant for the UIB.

615

616 **7 Conclusions**

617 We present a first comprehensive and systematic hydroclimatic trend analysis for the UIB
618 based on ten stream flow, six low-altitude manual and 12 high-altitude automatic weather
619 stations. Results suggest general narrowing of DTR throughout the year except for March and
620 May, which is significant in September followed by in February. Such year-round narrowing

of DTR is further found field significant for almost all sub-regions, and is mainly associated with either higher cooling in Tx than in Tn or cooling in Tx but warming in Tn.

Cooling at most of the stations is observed during the monsoon and the main glacier melt season (July-October), which is significant in September followed by in July. Further, locally observed cooling is found field significant for almost all sub-regions in July, September and October, and on a seasonal timescale, for autumn and summer. In contrast, well agreed local warming though mostly insignificantly observed in March, May and November is field significant in March for most of the sub-regions. For precipitation, March, spring and summer feature field significant drying for all the sub-regions except those within the karakoram while winter, autumn and September mostly feature wetting of high (drying of low) altitudinal sub-regions. Change pattern in discharge out of corresponding sub-regions seems more consistent with the field significant tendencies in temperature than in precipitation, where discharge is either falling or weakly rising (rising) in response to cooling (warming), particularly in the month of July (May). These findings though constrained by short and sparse observational dataset suggest distinct changes for the snow and glacier melt seasons, indicating at present strengthening of the nival but suppression of the glacial melt regime, altering the overall hydrology of the UIB. The presented findings largely contribute to the ongoing research on understanding the melt runoff dynamics within the UIB and in addressing the hydroclimatic explanation of the 'Karakoram Anomaly'.

Acknowledgement: The authors acknowledge the Water and Power Development Authority (WAPDA), Pakistan and the Pakistan Meteorological Department (PMD) for providing the hydroclimatic data. S. Hasson and J. Böhner acknowledge the support of BMBF, Germany's Bundle Project CLASH/Climate variability and landscape dynamics in Southeast-Tibet and the eastern Himalaya during the Late Holocene reconstructed from tree rings, soils and climate modeling. Authors also acknowledge the support from CliSAP/Cluster of excellence in the Integrated Climate System Analysis and Prediction.

References

Ahmad, Z., Hafeez, M., Ahmad, I.: Hydrology of mountainous areas in the upper Indus Basin, Northern Pakistan with the perspective of climate change, Environmental Monitoring and Assessment, 184, 9, pp 5255-5274, 2012.

Ali, G., Hasson, S., and Khan, A. M.: Climate Change: Implications and Adaptation of Water Resources in Pakistan, GCISC-RR-13, Global Change Impact Studies Centre (GCISC), Islamabad, Pakistan, 2009.

Archer, D. R. and Fowler, H. J.: Spatial and temporal variations in precipitation in the Upper Indus Basin, global teleconnections and hydrological implications, Hydrol. Earth Syst. Sci., 8, 47–61, doi:10.5194/hess-8-47-2004, 2004.

Archer, D. R.: Contrasting hydrological regimes in the upper Indus Basin, J. Hydrol., 274, 19–210, 2003.

Archer, D. R.: Hydrological implications of spatial and altitudinal variation in temperature in the Upper Indus Basin. Nord. Hydrol, 35 (3), 209–222, 2004.

Arendt, A., A. Bliss, T. Bolch, J.G. Cogley, A.S. Gardner, J.-O. Hagen, R. Hock, M. Huss, G. Kaser, C. Kienholz, W.T. Pfeffer, G. Moholdt, F. Paul, V. Radić, L. Andreassen, S. Bajracharya, N.E. Barrand, M. Beedle, E. Berthier, R. Bhambri, I. Brown, E. Burgess, D. Burgess, F. Cawkwell, T. Chinn, L. Copland, B. Davies, H. De Angelis, E. Dolgova, L. Earl, K. Filbert, R. Forester, A.G. Fountain, H. Frey, B. Giffen, N. Glasser, W.Q. Guo, S. Gurney, W. Hagg, D. Hall, U.K. Haritashya, G. Hartmann, C. Helm, S. Herreid, I. Howat, G. Kapustin, T. Khromova, M. König, J. Kohler, D. Kriegel, S. Kutuzov, I. Lavrentiev, R. LeBris, S.Y. Liu, J. Lund, W. Manley, R. Marti, C. Mayer, E.S. Miles, X. Li, B. Menounos, A. Mercer, N. Mölg, P. Mool, G. Nosenko, A. Negrete, T. Nuimura, C. Nuth, R. Pettersson, A. Racoviteanu, R. Ranzi, P. Rastner, F. Rau, B. Raup, J. Rich, H. Rott, A. Sakai, C. Schneider, Y. Seliverstov, M. Sharp, O. Sigurðsson, C. Stokes, R.G. Way, R. Wheate, S. Winsvold, G. Wolken, F. Wyatt, N. Zheltyhina, 2015, Randolph Glacier Inventory – A Dataset of Global Glacier Outlines: Version 5.0. Global Land Ice Measurements from Space, Boulder Colorado, USA. Digital Media. 2015.

Batura Investigations Group: The Batura Glacier in the Karakoram Mountains and its variations, Scientia Sinica, 22, 958–974, 1979.

Bengtsson, L., Hodges, I. K., and Roeckner, E.: Storm tracks and climate change, J. Climate, 19, 3518–3542, 2006.

Bhambri, R., Bolch, T., Kawishwar, P., Dobhal, D. P., Srivastava, D., and Pratap, B.: Heterogeneity in glacier response in the upper Shyok valley, northeast Karakoram, The Cryosphere, 7, 1385-1398, doi:10.5194/tc-7-1385-2013, 2013.

Bocchiola, D., and Diolaiuti, G.: Recent (1980–2009) evidence of climate change in the upper Karakoram, Pakistan, Theor Appl Climatol, 113:611–641, 2013.

Briffa, K. R., T. J. Osborn, F. H. Schweingruber, I. C. Harris, P. D. Jones, S. G. Shiyatov, and E. A. Vaganov,: Low frequency temperature variations from northern tree ring density network. J. Geophys. Res., 106, 2929–2941, 2001.

Brown, E.T., R. Bendick, D.L. Bourlès, V. Gaur, P. Molnar, G.M. Raisbeck, F. Yiou Early Holocene climate recorded in geomorphological features in Western Tibet Palaeogeogr. Palaeoclimatol. Palaeoecol., 199 (1–2) (2003), pp. 141–151 http://dx.doi.org/10.1016/S0031-0182(03)00501-7

Cannon, F., Carvalho, L. M. V., Jones, C., and Bookhagen, B.: Multi-annual variations in winter westerly disturbance activity affecting the Himalaya, Clim Dyn, 44:441–455, 2015. DOI 10.1007/s00382-014-2248-8

Cohen, J. L., Furtado, J. C., Barlow, M. A., Alexeev V. A., and Cherry, J. E.: Arctic warming, increasing snow cover and widespread boreal winter cooling, Environ. Res. Lett. 7 014007 (8pp), 2012.

699 Cook, E. R., Krusic, P. J. and Jones, P. D.: Dendroclimatic signals in long tree-ring
700 chronologies from the Himalayas of Nepal. Int. J. Climatol., 23, 707–732, 2003.

701 Douglas EM, Vogel RM, Kroll CN. Trends in floods and low flows in the United States:
702 impact of spatial correlation. Journal of Hydrology 240: 90–105, 2000.

703 Efron, B., Bootstrap methods: another look at the jackknife. Ann. Stat. 7 (1), 1-26, 1979.

704 Farhan, S. B., Zhang, Y., Ma, Y., Guo, Y. and Ma, N.: Hydrological regimes under the
705 conjunction of westerly and monsoon climates: a case investigation in the Astore Basin,
706 Northwestern Himalaya, Climate Dynamics, DOI: 10.1007/s00382-014-2409-9, 2014.

707 Forsythe, N., Hardy, A. J., Fowler, H. J., Blenkinsop, S., Kilsby, C. G., Archer, D. R., and
708 Hashmi, M. Z.: A Detailed Cloud Fraction Climatology of the Upper Indus Basin and Its
709 Implications for Near-Surface Air Temperature. J. Climate, 28, 3537–3556, 2015.

710 Fowler, H. J. and Archer, D. R.: Conflicting Signals of Climatic Change in the Upper
711 Indus Basin, J. Climate, 9, 4276–4293, 2006.

712 Fowler, H. J. and Archer, D. R.: Hydro-climatological variability in the Upper Indus
713 Basin and implications for water resources, Regional Hydrological Impacts of Climatic
714 Change – Impact Assessment and Decision Making (Proceedings of symposium S6,
715 Seventh IAHS Scientific Assembly at Foz do Iguaçu, Brazil, IAHS Publ., 295, 2005.

716 Gardelle, J., Berthier, E., Arnaud, Y., and Kääb, A.: Region–wide glacier mass balances
717 over the Pamir-Karakoram-Himalaya during 1999–2011, The Cryosphere, 7, 1263–1286,
718 doi:10.5194/tc-7-1263-2013, 2013.

719 Gioli, G., Khan, T., and Scheffran, J.: Climatic and environmental change in the
720 Karakoram: making sense of community perceptions and adaptation strategies. Regional
721 Environmental Change, 14, 1151-1162, 2013

722 Han, S., and Yang, Z.: Cooling effect of agricultural irrigation over Xinjiang, Northwest
723 China from 1959 to 2006, Environ. Res. Lett. 8 024039 doi:10.1088/1748-
724 9326/8/2/024039, 2013.

725 Hasson, S., Lucarini, V., Pascale, S., and Böhner, J.: Seasonality of the hydrological cycle
726 in major South and Southeast Asian river basins as simulated by PCMDI/CMIP3
727 experiments, Earth Syst. Dynam., 5, 67–87, doi:10.5194/esd-5-67-2014, 2014a.

728 Hasson, S., Lucarini, V., Khan, M. R., Petitta, M., Bolch, T., and Gioli, G.: Early 21st
729 century snow cover state over the western river basins of the Indus River system, Hydrol.
730 Earth Syst. Sci., 18, 4077-4100, doi:10.5194/hess-18-4077-2014, 2014b.

731 Hasson, S.; Pascale, S.; Lucarini, V.; Böhner, J.: Seasonal cycle of precipitation over
732 major river basins in South and Southeast Asia: A review of the CMIP5 climate models
733 data for present climate and future climate projections. Atmos. Res., 180, 42–63, 2016a.

734 Hasson, S., Seasonality of Precipitation over Himalayan Watersheds in CORDEX South
735 Asia and their Driving CMIP5 Experiments, Atmosphere, 7(10), 123, 2016b.
736 doi:10.3390/atmos7100123

737 Hasson, S.: Future Water Availability from Hindukush-Karakoram-Himalaya upper Indus
738 Basin under Conflicting Climate Change Scenarios. Climate. 26;4(3):40, 2016c.

739 Hasson, S., Gerlitz, L., Scholten, T., Schickhoff, U., and Böhner, J.: "Recent Climate
740 Change over High Asia", In Climate Change, Glacier Response, and Vegetation
741 Dynamics in the Himalaya, pp. 29-48. Springer International Publishing, 2016d.

742 Hewitt, K. The Karakoram anomaly? Glacier expansion and the 'elevation effect',
743 Karakoram Himalaya. Mt. Res. Dev. 25, 332–340, 2005.

744 Hewitt, K.: Glacier change, concentration, and elevation effects in the Karakoram
745 Himalaya, Upper Indus Basin, Mt. Res. Dev., 31, 188–200, doi:10.1659/MRD-
746 JOURNAL-D-11-00020.1, 2011.

747 Houze, R. A., Rasmussen, K. L., Medina, S., Brodzik, S. R., and Romatschke, U.:
748 Anomalous Atmospheric Events Leading to the Summer 2010 Floods in Pakistan, B. Am.
749 Meteorol. Soc., 92, 291–298, 2011.

750 Hu, Z. Z., Yang, S., and Wu, R. G.: Long-term climate variations in China and global
751 warming signals. J. Geophys. Res.,108, 4614, doi:10.1029/2003JD003651, 2003.

752 Immerzeel,W.W., Droogers, P., de Jong, S. M., and Bierkens, M. F. P.: Large-scale
753 monitoring of snow cover and runoff simulation in Himalayan river basins using remote
754 sensing, Remote Sens. Environ., 113, 40–49, 2009.

755 IPCC, 2013: Climate Change 2013: The Physical Science Basis. Contribution ofWorking
756 Group I to the Fifth Assessment Report of the Intergovernmental Panel on Climate
757 Change, edited by: Stocker, T. F., Qin, D., Plattner, G.-K., Tignor, M., Allen, S. K.,
758 Boschung, J., Nauels, A., Xia, Y., Bex, V., and Midgley, P. M., Cambridge University
759 Press, Cambridge, United Kingdom and New York, NY, USA, 1535 pp., 2013.

760 Jaagus, J.: Climatic changes in Estonia during the second half of the 20th century in
761 relationship with changes in large-scale atmospheric circulation. Theor Appl Climatol
762 83:77–88, 2006.

763 Kääb, A., Treichler, D., Nuth, C., and Berthier, E.: Brief Communication: Contending
764 estimates of 2003–2008 glacier mass balance over the Pamir–Karakoram–Himalaya, The
765 Cryosphere, 9, 557-564, doi:10.5194/tc-9-557-2015, 2015.

766 Kendall, M. G.: Rank Correlation Methods. Griffin, London, UK, 1975.

767 Khattak, M. S., Babel, M. S., and Sharif, M.: Hydrometeorological trends in the upper
768 Indus River Basin in Pakistan, Clim. Res., 46, 103–119, doi:10.3354/cr00957, 2011.

769 Klein Tank, AMG, Zwiers, FW, Zhang, X.: Guidelines on analysis of extremes in a
770 changing climate in support of informed decisions for adaptation (WCDMP-72, WMO-
771 TD/No.1500), WMO Publications Board, Geneva, Switzerland, 56 pp, 2009.

772 Kueppers, L. M., M. A. Snyder, and L. C. Sloan, Irrigation cooling effect: Regional
773 climate forcing by land-use change, Geophys. Res. Lett., 34, L03703,
774 doi:10.1029/2006GL028679. 2007.

775 Kulkarni, A. and von Storch, H.: Monte Carlo experiments on the effect of serial
776 correlation on the Mann–Kendall test of trend. Meteorologische Zeitschrift 4(2): 82–85,
777 1995.

778 Kumar, K. R., Kumar, K. K.and Pant, G. B.: Diurnal asymmetry of surface temperature
779 trends over India. Geophys. Res. Lett., 21, 677–680. 1994.

Lacombe, G., and McCartney, M.: Uncovering consistencies in Indian rainfall trends observed over the last half century, Climatic Change, 123:287–299, 2014.

Liu, X., and Chen, B.: Climatic warming in the Tibetan Plateau during recent decades. Int. J. Climatol., 20, 1729–1742, 2000.

Madhura, R. K., Krishnan, R., Revadekar, J. V., Mujumdar, M., Goswami, B. N.: Changes in western disturbances over the Western Himalayas in a warming environment, Clim Dyn, 44:1157–1168, 2015.

Mann, H. B.: Nonparametric tests against trend, Econometrica 13, 245–259, 1945.

MRI (Mountain Research Initiative) EDW (Elevation Dependent Warming) Working Group: Pepin N, Bradley RS, Diaz HF, Baraer M, Caceres EB, Forsythe N, Fowler H, Greenwood G, Hashmi MZ, Liu XD, Miller JR, Ning L, Ohmura A, Palazzi E, Rangwala I, Schöner W, Severskiy I, Shahgedanova M, Wang MB, Williamson SN, Yang DQ.: Elevation-dependent warming in mountain regions of the world. Nature Climate Change:5, DOI:10.1038/NCLIMATE2563, 2015.

Mukhopadhyay, B., and Khan, A.: Rising river flows and glacial mass balance in central Karakoram, Journal of Hydrology, 513, 26 Pages 192–203, 2014.

Mukhopadhyay, B., and Khan, A.: A reevaluation of the snowmelt and glacial melt in river flows within Upper Indus Basin and its significance in a changing climate, J. Hydrol., 119-132, 2015.

Ohlendorf, C., Niessenn, F., Weissert, H.:Glacial Varve thickness and 127 years of instrumental climate data: a comparison. Clim. Chang, 36:391–411, 1997.

Palazzi, E., von Hardenberg, J., Provenzale, A.: Precipitation in the Hindu-Kush Karakoram Himalaya: Observations and future scenarios. J Geophys Res Atmos 118:85, 100, DOI 10.1029/2012JD018697, 2013.

Revadekar, J. V., Hameed, S., Collins, D., Manton, M., Sheikh, M., Borgaonkar, H. P., Kothawale, D. R., Adnan, M., Ahmed, A. U., Ashraf, J., Baidya, S., Islam, N., Jayasinghearachchi, D., Manzoor, N., Premalal, K. H. M. S. and Shreshta, M. L, Impact of altitude and latitude on changes in temperature extremes over South Asia during 1971–2000. Int. J. Climatol., 33: 199–209. doi: 10.1002/joc.3418. 2013.

Río, S. D., Iqbal, M. A., Cano-Ortiz, A., Herrero, L., Hassan, A. and Penas, A.: Recent mean temperature trends in Pakistan and links with teleconnection patterns. Int. J. Climatol., 33: 277–290. doi: 10.1002/joc.3423, 2013

Rivard, C. and Vigneault, H.: Trend detection in hydrological series: when series are negatively correlated, Hydrol. Process. 23, 2737–2743, 2009.

Scherler, D., Bookhagen, B., Strecker, M. R.: Spatially variable response of Himalayan glaciers to climate change affected by debris cover. Nat. Geosci. 4, Nature Geoscience 4, 156–159, doi:10.1038/ngeo1068, 2011.

Sen, P. K.: Estimates of the regression coefficient based on Kendall's tau. J. Am. Statist. Assoc. 63, 1379–1389, 1968.

Sharma, K. P., Moore, B.and Vorosmarty, C. J.: Anthropogenic, climatic and hydrologic trends in the Kosi basin, Himalaya. Climatic Change, 47, 141–165, 2000.

Sheikh, M. M., Manzoor, N., Adnan, M., Ashraf, J., and Khan, A. M.: Climate Profile and Past Climate Changes in Pakistan, GCISC-RR-01, Global Change Impact Studies Centre (GCISC), Islamabad, Pakistan, ISBN: 978-969-9395-04-8, 2009.

SIHP: Snow and Ice Hydrology, Pakistan Phase-II Final Report to CIDA, IDRC File No. 88-8009-00 International Development Research Centre, Ottawa, Ontario, Canada, KIG 3H9, Report No. IDRC.54, 1997.

Syed, F. S., Giorgi, F., Pal, J. S., and King, M. P.: Effect of remote forcing on the winter precipitation of central southwest Asia Part 1: Observations, Theor. Appl. Climatol., 86, 147–160, doi:10.1007/s00704-005-0217-1, 2006.

Tabari, H., and Talaee, P. H.: Recent trends of mean maximum and minimum air temperatures in the western half of Iran, Meteorol. Atmos. Phys.,111:121–131, 2011.

Tahir, A.A.; Adamowski, J.F.; Chevallier, P.; Haq, A.U.; Terzago, S. Comparative assessment of spatiotemporal snow cover changes and hydrological behavior of the Gilgit, Astore and Hunza River basins (Hindukush-Karakoram-Himalaya region, Pakistan). Meteorol. Atmos. Phys. 2016, doi:10.1007/s00703-016-0440-6.

Theil, H.: A rank-invariant method of linear and polynomial regression analysis, I, II, III. Nederl. Akad. Wetensch, Proc. 53, 386–392, 512–525, 1397–1412, Amsterdam, 1950.

Vogel, R.M., and Kroll, C.N.: Low-flow frequency analysis using probability plot correlation coefficients, J. Water Res. Plann. Mgmt, 115 (3) (1989), pp. 338–357, 1989.

Von Storch, H.: Misuses of statistical analysis in climate research. In Analysis of Climate Variability: Applications of Statistical Techniques, von Storch H, Navarra A (eds). Springer-Verlag: Berlin; 11–26, 1995.

Wake, C. P.: Glaciochemical investigations as a tool to determine the spatial variation of snow accumulation in the Central Karakoram, Northern Pakistan, Ann. Glaciol., 13, 279–284, 1989.

Wake, C. P.: Snow accumulation studies in the central Karakoram, Proc. Eastern Snow Conf. 44th Annual Meeting Fredericton, Canada, 19–33, 1987.

Wang XL, Feng Y.: RHtestsV3 user manual, report, 26 pp, Clim. Res. Div., Atmos. Sci. and Technol. Dir., Sci. and Technol. Branch, Environ. Canada, Gatineau, Quebec, Canada. Available at http://etccdi.pacificclimate.org/software.shtml, (last access: 15 November 2014), 2009.

Wang, F., Zhang, C., Peng, Y. and Zhou, H.: Diurnal temperature range variation and its causes in a semiarid region from 1957 to 2006. Int. J. Climatol., 34: 343–354. doi: 10.1002/joc.3690, 2014.

Wang, X. L. and Swail, V. R.: Changes of Extreme Wave Heights in Northern Hemisphere Oceans and Related Atmospheric Circulation Regimes, J. Clim., 14, 2204-2221, 2001.

Wang, X. L.: Penalized maximal F-test for detecting undocumented mean shifts without trend-change. J. Atmos. Oceanic Tech., 25 (No. 3), 368-384. DOI:10.1175/2007JTECHA982.1, 2008.

Wendler, G. and Weller, G.: 'A Heat-Balance Study on McCall Glacier, Brooks Range, Alaska: A Contribution to the International Hydrological Decade', J. Glaciol. 13, 13–26. 1974.

Winiger, M., Gumpert, M., and Yamout, H.: Karakorum–Hindukush–western Himalaya: assessing high-altitude water resources, Hydrol. Process., 19, 2329–2338, doi:10.1002/hyp.5887, 2005.

Wu, H., Soh, L-K., Samal, A., Chen, X-H: Trend Analysis of Streamflow Drought Events n Nebraska, Water Resour. Manage., DOI 10.1007/s11269-006-9148-6, 2008.

Yadav, R. R., Park, W.-K., Singh, J. and Dubey, B.: Do the western Himalayas defy global warming? Geophys. Res. Lett., 31, L17201, doi:10.1029/2004GL020201. 2004.

Yue, S. and Wang, C. Y.: Regional streamflow trend detection with consideration of both temporal and spatial correlation. Int. J. Climatol., 22: 933–946. doi: 10.1002/joc.781. 2002.

Yue, S., Pilon, P., Phinney, B. and Cavadias, G.: The influence of autocorrelation on the ability to detect trend in hydrological series, Hydrol. Process. 16, 1807–1829, 2002.

Yue, S., Pilon, P., Phinney, B.: Canadian streamflow trend detection: impacts of serial and cross-correlation, Hydrological Sciences Journal, 48:1, 51-63, DOI: 10.1623/hysj.48.1.51.43478, 2003.

Zhai, P. Zhang, X., Wan, H., and Pan, X.: Trends in Total Precipitation and Frequency of Daily Precipitation Extremes over China. J. Climate, 18, 1096–1108, 2005. doi: http://dx.doi.org/10.1175/JCLI-3318.1

Zhang, X., Vincent, L. A., Hogg, W.D. and Niitsoo, A.: Temperature and precipitation trends in Canada during the 20th century, Atmosphere-Ocean, 38:3, 395-429, 2000.

884 Table 1: Characteristics of the gauged and derived regions of UIB. Note: *Including nearby Skardu and Gilgit stations for the Karakoram and
885 Deosai station for the UIB-Central regions. Derived time series are limited to a common length of used gauges' record, thus their statistics.

S. No.	Watershed/ Tributary	Designated Discharge sites	Expression for deriving approximated Discharge	Designated Name of the Region	Area (km^2)	Glacier Cover (km^2)	% Glacier Cover	% of UIB Glacier Aboded	Elevation Range (m)	Mean Discharge (m^3s^{-1})	% of UIB Discharge	No of Met Stations
1	Indus	Kharmong		UIB-East	69,355	2,643	4	14	2250-7027	451	18.8	1
2	Shyok	Yogo		Eastern-Karakoram	33,041	7,783	24	42	2389-7673	360	15.0	1
3	Shigar	Shigar		Central-Karakoram	6,990	2,107	30	11	2189-8448	206	8.6	1
4	Indus	Kachura		Indus at Kachura	113,035	12,397	11	68	2149-8448	1078	44.8	
5	Hunza	Dainyor Bridge		Western-Karakoram	13,734	3,815	28	21	1420-7809	328	13.6	4
6	Gilgit	Gilgit		Hindukush	12,078	818	7	4	1481-7134	289	12.0	5
7	Gilgit	Alam Bridge		UIB-West-upper	27,035	4,676	21	25	1265-7809	631	27.0	9
8	Indus	Partab Bridge		Indus at Partab	143,130	17,543	12	96	1246-8448	1788	74.3	
9	Astore	Doyian		Astore at Doyian	3,903	527	14	3	1504-8069	139	5.8	3
10	**UIB**	**Besham Qila**		**UIB**	**163,528**	**19,370**	**12**	**100**	**569-8448**	**2405**	**100.0**	**18**
11			4 – 2 – 1	Shigar-region						305	12.7	
12			2 + 3 + 5	Karakoram	53,765	13,705	25	75	1420-8448	894	37.2	*8
13			2 + 11 + 5	derived Karakoram						993	41.3	
14			4 – 1	UIB-Central	43,680	9,890	23	54	2189-8448	627	26.1	*4
15			10 – 4	UIB-West	50,500	5,817	13	32	569-7809	1327	55.2	14
16			10 – 4 – 7	UIB-West-lower	23,422	1,130	7	6	569-8069	696	28.9	5
17			1 + 16	Himalaya	92,777	3,773	5	20	569-8069	1147	47.7	7

Table 2: Meteorological stations and their attributes. Inhomogeneity is found only in Tn over full period of record. Note: (*) represents inhomogeneity only over the 1995-2012 period.

S. No.	Station Name	Period From	Period To	Agency	Latitude (degrees)	Longitude (degrees)	Altitude (meters)	Inhomogeneity at
1	Chillas	01/01/1962	12/31/2012	PMD	35.42	74.10	1251	2009/03
2	Bunji	01/01/1961	12/31/2012	PMD	35.67	74.63	1372	1977/11
3	Skardu	01/01/1961	12/31/2012	PMD	35.30	75.68	2210	
4	Astore	01/01/1962	12/31/2012	PMD	35.37	74.90	2168	1981/08
5	Gilgit	01/01/1960	12/31/2012	PMD	35.92	74.33	1460	2003/10*
6	Gupis	01/01/1961	12/31/2010	PMD	36.17	73.40	2156	1988/12
								1996/07*
7	Khunjrab	01/01/1995	12/31/2012	WAPDA	36.84	75.42	4440	
8	Naltar	01/01/1995	12/31/2012	WAPDA	36.17	74.18	2898	2010/09*
9	Ramma	01/01/1995	09/30/2012	WAPDA	35.36	74.81	3179	
10	Rattu	03/29/1995	03/16/2012	WAPDA	35.15	74.80	2718	
11	Hushe	01/01/1995	12/31/2012	WAPDA	35.42	76.37	3075	
12	Ushkore	01/01/1995	12/31/2012	WAPDA	36.05	73.39	3051	
13	Yasin	01/01/1995	10/06/2010	WAPDA	36.40	73.50	3280	
14	Ziarat	01/01/1995	12/31/2012	WAPDA	36.77	74.46	3020	
15	Dainyor	01/15/1997	07/31/2012	WAPDA	35.93	74.37	1479	
16	Shendoor	01/01/1995	12/28/2012	WAPDA	36.09	72.55	3712	
17	Deosai	08/17/1998	12/31/2011	WAPDA	35.09	75.54	4149	
18	Shigar	08/27/1996	12/31/2012	WAPDA	35.63	75.53	2367	

Table 3. SWHP WAPDA stream flow gauges given in the downstream order along with their characteristics and their periods of record analyzed**. ***Gauge is not operational after 2001.

S. No.	Gauged River	Discharge Gauging Site	Period From	Period To	Latitude (degrees)	Longitude (degrees)	Height (meters)
1	Indus	Kharmong	May-82	Dec-11	34.93	76.21	2542
2	Shyok	Yogo	Jan-74	Dec-11	35.18	76.10	2469
3	Shigar	Shigar*	Jan-85	Dec-98 & 2001	35.33	75.75	2438
4	Indus	Kachura	Jan-70	Dec-11	35.45	75.41	2341
5	Hunza	Dainyor	Jan-66	Dec-11	35.92	74.37	1370
6	Gilgit	Gilgit	Jan-70	Dec-11	35.92	74.30	1430
7	Gilgit	Alam Bridge	Jan-74	Dec-12	35.76	74.59	1280
8	Indus	Partab Bridge	Jan-62	Dec-07	35.73	74.62	1250
9	Astore	Doyian	Jan-74	Aug-11	35.54	74.70	1583
10	UIB	Besham Qila	Jan-69	Dec-12	34.92	72.88	580

Table 4. Trend for Tx, Tn and DTR in °C (per unit time) at monthly to annual timescales over the period 1995-2012. Note: stations are given in top to bottom altitude order. Slopes significant at 90% level are given in bold.

Vars.	Stations	Jan	Feb	Mar	Apr	May	Jun	Jul	Aug	Sep	Oct	Nov	Dec	DJF	MAM	JJA	SON	Ann.
Tx	Khunjrab	0.01	-0.01	0.10	0.03	0.12	-0.01	-0.09	0.06	-0.16	0.01	0.12	0.07	0.05	0.07	-0.05	0.04	0.04
	Deosai	0.02	-0.05	0.07	-0.01	0.06	0.01	-0.19	-0.01	0.00	0.02	0.06	0.05	0.08	0.06	0.03	0.02	0.06
	Shendure	-0.17	**-0.09**	0.01	-0.03	-0.06	-0.10	**-0.13**	**-0.07**	**-0.22**	-0.06	0.04	-0.11	-0.08	-0.06	**-0.11**	-0.05	-0.05
	Yasin	0.00	-0.03	**0.13**	-0.02	0.10	0.03	-0.16	-0.08	**-0.35**	0.12	-0.02	-0.10	0.03	0.08	-0.06	-0.01	0.05
	Rama	-0.06	-0.07	0.02	**-0.11**	0.14	0.04	-0.11	-0.09	**-0.29**	-0.10	0.01	0.00	-0.04	-0.04	**-0.07**	-0.07	**-0.08**
	Hushe	-0.05	-0.01	0.09	0.00	0.17	-0.06	-0.09	0.02	**-0.20**	-0.09	0.01	0.03	0.02	0.03	-0.02	-0.03	-0.03
	Ushkore	-0.04	-0.02	0.10	0.03	0.25	-0.01	-0.12	-0.06	**-0.22**	-0.05	0.06	-0.01	0.02	0.08	-0.05	-0.02	-0.01
	Ziarat	0.00	-0.01	0.12	-0.02	0.13	0.09	-0.11	-0.03	**-0.21**	-0.04	0.09	0.04	0.06	0.06	-0.02	-0.04	0.01
	Naltar	-0.04	-0.04	0.10	-0.03	0.10	0.03	-0.12	-0.03	**-0.19**	0.03	-0.01	0.01	-0.02	0.07	-0.03	-0.05	0.00
	Rattu	**-0.16**	-0.10	0.04	-0.03	0.11	0.14	-0.06	-0.05	-0.17	-0.23	0.04	-0.15	**-0.12**	-0.03	0.01	-0.03	**-0.07**
	Shigar	-0.04	-0.08	-0.02	-0.08	-0.38	-0.15	-0.08	0.03	-0.01	-0.09	0.11	0.01	-0.02	-0.09	**-0.09**	-0.02	-0.02
	Skardu	0.10	0.08	0.12	0.04	0.04	-0.08	**-0.10**	0.06	**-0.23**	-0.10	-0.04	-0.05	-0.02	0.13	-0.07	**-0.09**	-0.02
	Astore	0.09	0.00	**0.20**	0.03	0.18	0.06	-0.05	-0.03	**-0.15**	-0.11	0.05	0.04	0.08	**0.15**	-0.01	-0.05	0.02
	Gupis	-0.05	0.03	**0.27**	0.11	0.20	0.01	-0.09	-0.13	-0.09	0.12	0.12	0.03	0.11	0.20	0.03	0.03	0.07
	Dainyor	-0.04	-0.08	**0.23**	-0.02	0.15	-0.19	**-0.18**	0.01	-0.15	-0.04	0.10	-0.07	**-0.06**	0.14	-0.08	-0.01	-0.02
	Gilgit	0.09	-0.07	0.12	0.03	0.15	0.02	**-0.15**	**-0.08**	**-0.31**	-0.07	0.07	-0.05	-0.04	0.06	-0.05	**-0.08**	-0.05
	Bunji	0.09	-0.08	0.13	0.04	0.11	0.07	-0.01	0.04	**-0.22**	-0.12	-0.01	-0.08	0.00	0.11	0.02	-0.07	-0.02
	Chilas	0.09	-0.03	**0.16**	0.01	0.13	0.01	**-0.15**	-0.06	**-0.24**	0.00	0.03	-0.06	-0.05	0.08	**-0.07**	-0.05	-0.06
Tn	Khunjrab	**0.15**	**0.26**	**0.16**	0.03	0.18	-0.02	-0.04	0.00	0.01	0.05	**0.17**	0.10	**0.21**	0.08	-0.01	0.06	**0.09**
	Deosai	0.02	0.09	**0.21**	0.00	0.01	0.00	0.03	-0.02	-0.08	0.03	0.09	0.00	0.06	0.10	-0.02	0.05	**0.10**
	Shendure	0.04	-0.03	0.10	0.06	0.05	0.00	**-0.06**	0.00	-0.10	-0.01	0.10	0.08	0.09	0.07	-0.03	0.01	0.05
	Yasin	0.09	0.07	0.12	0.02	0.10	0.01	-0.11	-0.05	**-0.21**	0.10	0.04	-0.08	0.06	**0.11**	-0.04	0.03	**0.08**
	Rama	-0.08	0.10	0.05	0.02	0.06	0.01	0.00	0.01	-0.09	0.00	0.11	0.07	-0.02	0.03	0.03	0.02	0.02
	Hushe	0.00	**0.14**	0.08	0.02	0.14	-0.04	-0.08	0.04	**-0.09**	-0.04	0.04	0.01	0.06	0.06	-0.01	0.01	0.01
	Ushkore	-0.06	0.05	0.08	0.09	0.13	0.00	-0.04	-0.02	**-0.16**	-0.09	0.08	0.01	0.00	0.08	0.01	-0.01	0.00
	Ziarat	0.12	**0.23**	0.11	0.04	0.04	0.04	**-0.08**	0.01	**-0.10**	-0.01	0.09	0.09	**0.17**	0.07	0.00	0.01	**0.06**
	Naltar	-0.01	0.08	0.10	0.02	-0.01	-0.03	**-0.10**	-0.01	**-0.07**	0.00	-0.03	0.00	-0.07	0.10	-0.03	-0.01	0.04
	Rattu	-0.05	0.10	-0.08	-0.02	0.06	0.05	-0.07	0.01	-0.12	-0.02	0.07	0.01	0.04	-0.03	0.01	**-0.08**	-0.04
	Shigar	0.03	0.02	-0.01	-0.03	-0.21	-0.09	-0.07	0.05	0.07	-0.11	0.05	0.04	0.01	-0.02	-0.06	-0.01	0.01
	Skardu	-0.03	0.08	-0.02	-0.02	-0.07	-0.11	-0.15	-0.08	-0.10	**-0.12**	**-0.14**	-0.11	-0.18	-0.01	**-0.12**	**-0.16**	**-0.08**
	Astore	0.01	0.09	0.05	0.03	-0.02	0.02	-0.07	0.01	**-0.10**	-0.05	0.05	-0.08	0.06	**0.11**	-0.01	-0.03	-0.02
	Gupis	-0.15	-0.03	**0.19**	0.11	0.09	0.03	-0.04	0.04	-0.07	-0.03	-0.12	-0.14	-0.11	0.14	-0.04	-0.09	0.01
	Dainyor	-0.13	0.01	**0.13**	0.01	0.11	-0.04	**-0.17**	**0.03**	-0.06	-0.02	-0.06	-0.05	0.01	0.07	-0.03	-0.04	0.01
	Gilgit	0.03	0.10	0.06	0.04	0.04	0.05	-0.01	**0.26**	**0.30**	0.05	0.09	-0.01	0.08	**0.07**	0.06	0.19	**0.08**
	Bunji	0.01	0.03	0.05	0.03	0.02	0.04	-0.01	0.17	0.01	0.03	**0.13**	0.00	0.02	0.05	0.06	0.04	0.03
	Chilas	-0.09	**-0.18**	0.01	-0.07	0.02	-0.05	-0.11	-0.08	**-0.21**	-0.10	0.00	-0.06	-0.15	-0.05	**-0.07**	**-0.11**	-0.07
DTR	Khunjrab	-0.10	**-0.25**	-0.30	-0.19	**-0.24**	-0.08	**-0.13**	**-0.11**	**-0.11**	-0.04	-0.03	-0.05	**-0.17**	-0.18	-0.04	**-0.04**	**-0.08**
	Deosai	0.07	-0.09	0.01	0.11	-0.05	0.05	0.16	**0.19**	0.01	0.02	-0.01	0.03	0.01	0.00	0.13	0.01	**0.13**
	Shendure	-0.06	-0.09	-0.26	**-0.29**	-0.17	-0.08	-0.03	-0.05	**-0.09**	-0.07	-0.05	-0.24	-0.12	**-0.20**	-0.10	-0.06	-0.15
	Yasin	-0.13	**-0.23**	-0.05	**-0.15**	-0.12	**-0.20**	-0.13	-0.11	**-0.22**	**-0.58**	-0.24	-0.19	**-0.08**	-0.07	**-0.14**	**-0.25**	**-0.12**
	Rama	-0.05	**-0.16**	-0.04	**-0.11**	-0.04	-0.02	**-0.15**	**-0.13**	**-0.27**	-0.20	-0.08	-0.07	**-0.09**	-0.07	**-0.07**	**-0.13**	**-0.08**
	Hushe	**-0.08**	**-0.17**	-0.01	-0.05	-0.02	0.00	-0.03	-0.02	**-0.07**	0.00	-0.03	-0.01	**-0.10**	-0.01	-0.02	**-0.03**	**-0.04**
	Ushkore	0.00	-0.06	-0.02	-0.08	-0.01	-0.05	-0.01	-0.02	**-0.08**	-0.01	-0.02	-0.03	-0.03	-0.02	-0.03	**-0.03**	**-0.03**
	Ziarat	-0.09	**-0.26**	0.02	-0.02	0.01	-0.01	-0.05	-0.01	**-0.10**	-0.03	-0.03	-0.12	-0.13	0.03	-0.02	**-0.05**	**-0.06**
	Naltar	-0.06	**-0.15**	0.02	-0.06	0.06	-0.02	-0.02	-0.02	-0.09	-0.03	-0.03	-0.13	**-0.08**	0.00	-0.01	-0.06	**-0.05**
	Rattu	-0.10	**-0.16**	-0.04	**-0.10**	0.02	-0.04	-0.09	**-0.11**	**-0.18**	**-0.16**	-0.18	**-0.15**	**-0.12**	-0.01	**-0.04**	-0.10	**-0.05**
	Shigar	0.08	0.00	-0.05	0.00	0.01	0.03	-0.03	-0.01	-0.07	0.01	**0.08**	0.07	0.07	0.03	-0.06	0.00	-0.07
	Skardu	-0.04	**-0.14**	0.06	0.01	**0.13**	0.06	-0.01	-0.02	**-0.21**	0.04	0.03	0.14	-0.07	0.07	-0.01	-0.01	0.00
	Astore	-0.02	-0.13	0.13	0.00	0.05	0.00	-0.03	-0.07	**-0.08**	0.03	-0.03	0.04	-0.09	0.06	-0.02	-0.05	-0.01
	Gupis	0.04	0.00	0.15	-0.01	0.10	-0.01	-0.03	-0.10	-0.05	**0.16**	0.16	0.15	**0.13**	0.07	-0.06	0.09	0.09
	Dainyor	-0.05	-0.09	0.06	-0.11	-0.21	-0.19	-0.11	-0.07	-0.10	-0.44	-0.01	-0.07	-0.09	-0.07	-0.23	-0.12	-0.19
	Gilgit	-0.13	**-0.19**	0.05	-0.02	0.10	-0.13	**-0.27**	**-0.26**	**-0.87**	-0.18	-0.09	-0.02	-0.11	-0.03	**-0.15**	**-0.25**	**-0.18**
	Bunji	-0.04	**-0.14**	0.05	0.03	0.04	-0.01	-0.03	-0.04	**-0.27**	-0.03	-0.16	-0.10	-0.07	0.06	-0.01	**-0.14**	-0.05
	Chilas	0.07	0.09	**0.21**	0.11	**0.13**	0.03	-0.04	0.04	0.00	0.08	0.01	0.04	0.10	**0.14**	0.02	0.02	0.02

Table 5. Same as Table 4. Here, slopes for P are in mm and for Q in m^3s^{-1}. Hydrometric gauges are given in the downstream order.

Vars.	Stations	Jan	Feb	Mar	Apr	May	Jun	Jul	Aug	Sep	Oct	Nov	Dec	DJF	MAM	JJA	SON	Ann.
Tavg	Khunjrab	0.13	0.09	0.13	0.05	0.19	0.00	-0.06	0.06	-0.13	0.05	**0.17**	0.10	**0.15**	0.09	-0.03	0.06	0.06
	Deosai	0.06	0.01	**0.15**	0.00	0.07	0.01	-0.07	0.03	-0.05	0.02	0.08	0.01	**0.10**	0.06	0.03	0.04	**0.07**
	Shendure	-0.05	-0.05	0.05	0.02	0.02	-0.05	-0.10	-0.05	**-0.15**	-0.04	0.06	-0.03	0.01	-0.04	-0.05	-0.02	0.01
	Yasin	0.02	0.01	**0.13**	0.01	0.06	0.04	-0.19	-0.07	**-0.27**	0.11	0.01	-0.08	0.04	0.13	-0.05	0.02	0.06
	Rama	-0.12	0.02	0.05	-0.06	0.07	0.01	-0.03	-0.03	**-0.19**	-0.09	0.05	0.02	0.02	0.00	0.00	-0.01	-0.04
	Hushe	-0.03	0.05	0.06	0.02	0.14	-0.05	-0.07	0.02	**-0.13**	-0.07	0.03	0.04	0.01	0.06	-0.01	0.00	-0.01
	Ushkore	-0.07	0.00	0.08	0.05	0.21	0.00	-0.03	-0.03	**-0.17**	-0.09	0.06	0.01	0.04	0.09	-0.01	-0.02	0.01
	Ziarat	0.04	**0.11**	0.10	0.00	0.09	0.06	-0.09	-0.03	**-0.15**	-0.03	0.09	0.03	**0.08**	**0.07**	-0.02	0.00	0.05
	Naltar	-0.03	0.01	0.08	-0.05	-0.11	-0.07	**-0.12**	-0.06	**-0.17**	0.00	-0.03	0.01	-0.13	0.07	-0.04	-0.04	0.01
	Rattu	-0.11	-0.01	-0.05	-0.04	0.09	0.10	-0.04	0.00	-0.18	-0.07	0.04	-0.10	-0.06	0.03	0.00	-0.05	-0.05
	Shigar	0.05	-0.02	0.00	-0.06	-0.30	-0.13	-0.13	0.04	0.04	-0.14	0.07	0.03	0.01	-0.04	-0.07	-0.01	0.00
	Skardu	0.02	0.11	0.07	0.01	0.02	-0.10	**-0.15**	0.04	**-0.17**	**-0.11**	**-0.06**	-0.07	-0.11	0.06	-0.12	**-0.12**	**-0.07**
	Astore	0.10	0.03	**0.12**	0.01	0.13	0.03	-0.05	0.00	**-0.14**	-0.09	0.03	-0.01	0.05	**0.13**	-0.02	-0.03	0.01
	Gupis	-0.08	-0.06	**0.22**	0.09	0.13	0.00	-0.05	-0.05	-0.08	0.06	0.04	-0.07	0.02	**0.14**	0.02	-0.01	0.03
	Dainyor	-0.06	-0.02	**0.22**	-0.01	0.18	-0.08	**-0.15**	0.02	-0.11	-0.04	0.04	-0.09	-0.05	0.11	-0.04	-0.04	0.00
	Gilgit	0.02	0.01	0.11	0.03	0.06	0.04	-0.06	0.05	-0.09	0.00	**0.08**	0.05	0.03	0.08	-0.02	0.00	0.03
	Bunji	0.06	-0.02	0.06	0.02	0.05	0.02	0.00	0.09	-0.07	0.03	0.06	-0.06	0.03	0.08	0.06	0.00	0.01
	Chilas	-0.02	-0.14	0.06	-0.02	0.16	-0.03	**-0.12**	-0.07	**-0.19**	-0.07	0.01	-0.06	**-0.09**	0.03	**-0.06**	**-0.08**	-0.07
P	Khunjrab	**3.64**	2.59	-2.21	-1.55	-1.47	0.10	0.35	0.80	1.82	-1.04	0.93	2.34	**8.86**	-9.09	-1.74	1.65	6.14
	Deosai	0.07	1.28	**-1.42**	-0.66	-1.27	-0.89	-0.40	-1.00	-0.77	-0.42	-0.81	-0.32	1.40	-4.50	0.00	-1.99	-7.87
	Shendure	**1.54**	**2.75**	1.35	2.13	0.60	**2.12**	**1.83**	**1.38**	**1.45**	1.24	1.40	**1.20**	**5.71**	**4.50**	**4.82**	**3.58**	**29.53**
	Yasin	1.33	**1.86**	0.59	0.25	1.22	-0.50	**1.45**	0.02	0.92	-0.21	0.06	**2.74**	**6.09**	0.60	1.32	0.26	11.70
	Rama	0.77	0.00	-6.50	**-8.55**	**-4.52**	**-2.16**	**-2.35**	**-1.89**	**-1.44**	**-2.05**	-3.74	-2.03	7.00	**-25.44**	**-8.41**	**-14.60**	**-43.92**
	Hushe	0.65	0.24	-1.23	-0.30	-1.97	-1.21	-1.71	-0.60	0.73	-0.64	0.11	0.72	**3.47**	-4.51	-4.28	0.70	-5.54
	Ushkore	0.56	-0.59	**-2.33**	-1.02	-1.97	-0.93	0.00	-0.09	1.01	**-0.61**	-0.48	0.09	-0.13	-4.57	-1.54	-0.42	-3.83
	Ziarat	-0.91	-0.56	**-4.18**	**-5.28**	-1.83	0.25	-0.67	-0.18	**1.20**	-0.58	-0.43	-0.61	-3.59	**-9.10**	-1.71	-0.21	**-16.32**
	Naltar	3.75	8.41	-4.49	-0.36	-2.75	**-2.17**	0.43	-2.33	1.32	-0.36	-0.70	1.35	**19.43**	-8.39	-0.99	2.42	-0.28
	Rattu	**1.36**	**2.13**	0.08	0.36	0.26	0.53	**0.91**	0.75	**0.95**	**0.84**	**0.69**	**1.53**	**4.43**	1.23	1.81	**2.36**	10.64
	Shigar	-0.24	-0.89	-1.07	-2.62	-2.05	-0.33	1.75	0.80	**2.40**	1.13	0.18	1.49	-1.67	**-8.36**	0.78	**3.08**	-7.04
	Skardu	-0.64	1.62	0.60	0.19	-0.74	-0.47	-0.07	-0.44	0.46	0.00	0.00	0.20	0.41	0.89	-1.26	0.49	1.29
	Astore	0.00	0.41	0.12	**-1.41**	-0.48	-0.16	-0.08	-0.29	0.57	0.00	0.00	0.29	1.50	-1.36	-1.63	0.34	-0.16
	Gupis	0.65	**0.97**	**0.81**	0.38	-0.06	**-1.33**	**-1.07**	-0.49	0.06	0.35	0.26	**0.89**	2.81	0.29	**-3.49**	0.43	4.46
	Dainyor	-0.21	0.42	**0.51**	**0.55**	**0.67**	**1.24**	0.91	-0.71	-0.39	0.00	0.00	0.00	**1.68**	**1.81**	3.09	-0.34	6.69
	Gilgit	0.98	0.45	**-1.94**	-1.34	-1.57	-0.73	0.29	**-3.99**	0.32	0.00	0.00	0.30	0.00	**-9.39**	**-9.60**	-0.92	**-20.31**
	Bunji	0.01	-0.10	**-1.06**	**-2.34**	0.17	0.20	-0.34	-0.22	0.56	-0.01	0.00	0.11	-0.47	-2.68	-0.51	0.06	0.09
	Chilas	0.00	0.13	-0.14	-1.56	0.16	0.29	-0.51	0.13	**1.37**	-0.10	0.00	0.07	0.22	-0.81	-0.80	1.86	0.53
Q	UIB-East	**-0.80**	0.00	0.04	0.11	-4.19	2.00	-1.65	6.70	-4.74	-5.45	**-2.46**	**-1.37**	**-0.75**	-2.64	-2.62	-0.86	-1.73
	Eastern-Kara.	0.06	0.08	-0.10	0.00	1.96	0.96	**-22.97**	0.92	-8.84	-1.06	0.50	-0.09	0.29	0.67	0.30	-4.41	-0.95
	Central-Kara.	0.96	1.28	1.56	-0.84	3.74	-8.94	**-37.93**	-9.08	-5.98	0.71	2.50	**2.76**	1.13	1.13	-21.61	1.10	-1.56
	Kachura	0.33	1.39	**1.06**	-0.33	-2.08	-22.50	**-50.04**	-16.74	-4.25	-2.18	0.59	2.64	0.46	-0.81	-18.90	-2.63	-4.97
	UIB-Central	**2.19**	1.81	2.02	-0.84	6.89	-18.08	**-43.79**	-20.20	-4.88	1.05	**4.38**	**2.34**	**2.00**	1.79	-18.34	2.01	-2.47
	Western-Kara.	1.20	1.00	1.50	**2.00**	0.59	12.09	-4.53	-4.09	**6.40**	**3.50**	**3.82**	**2.03**	**1.88**	1.00	-1.64	**5.43**	2.50
	Karakoram	1.88	2.00	1.33	1.00	-5.82	-7.80	**-64.97**	-37.17	-9.48	0.60	**8.97**	**5.97**	**1.65**	0.11	-24.43	5.64	-3.90
	Hindukush	0.87	0.26	0.15	1.27	2.05	3.49	-6.61	**14.02**	**7.03**	2.17	1.82	1.06	0.75	1.00	3.94	4.44	4.00
	UIB-WU	1.24	**1.02**	1.39	**2.38**	**16.85**	12.38	-25.48	-15.50	-1.28	0.69	0.98	0.52	0.55	**7.76**	-3.68	0.45	-1.25
	Astore	0.05	0.00	0.22	0.50	7.65	4.26	-3.01	5.00	-1.00	-1.11	-0.67	0.00	0.00	2.20	1.97	-0.89	2.16
	Partab_Bridge	1.00	-0.13	3.60	8.80	63.22	-34.86	-39.86	-67.33	29.65	0.69	8.89	15.12	8.40	36.29	-67.00	9.81	-12.40
	UIB-WL	1.88	0.41	6.39	-0.52	41.58	**59.50**	28.19	**81.58**	**30.99**	16.18	5.17	2.33	1.92	19.90	**65.53**	**16.02**	**25.44**
	UIB-WL-Partab	-3.00	0.80	-4.38	-0.82	**87.89**	51.53	9.00	17.67	2.71	-12.24	1.40	-6.00	-3.74	28.32	47.93	-3.00	18.94
	UIB_West	2.45	1.37	5.43	2.42	**61.35**	54.89	0.21	42.93	**28.24**	**13.68**	**5.87**	1.38	2.00	**23.43**	44.18	**17.71**	**22.17**
	Himalaya	0.30	-0.32	4.10	0.91	43.99	62.23	12.43	83.33	22.43	9.97	2.32	0.23	1.17	26.64	**57.88**	7.75	**24.66**
	UIB	1.82	**5.09**	5.37	-2.50	11.35	14.67	-46.60	41.71	35.22	10.17	5.29	0.75	1.91	15.72	-1.40	19.35	4.25

909 Table 6. Long-term trends (1961-2012) in Tx, Tn, Tavg, DTR and P at monthly to annual timescales in
910 respective units as per given in Tables 4 and 5. Note: 'Kara' refers to Karakoram

Vars.	Stations/ sub-regions	Jan	Feb	Mar	Apr	May	Jun	Jul	Aug	Sep	Oct	Nov	Dec	DJF	MAM	JJA	SON	Ann.
Tx	Skardu	**0.07**	**0.06**	**0.06**	**0.05**	**0.07**	0.02	0.01	0.00	0.02	**0.03**	**0.06**	**0.06**	**0.05**	**0.07**	0.01	**0.04**	**0.04**
	Astore	0.02	0.01	**0.06**	**0.04**	**0.05**	-0.01	-0.01	-0.02	0.00	0.02	**0.03**	**0.04**	**0.02**	**0.06**	-0.01	**0.02**	**0.02**
	Gupis	0.02	0.02	0.03	**0.04**	**0.06**	-0.02	-0.02	-0.03	-0.01	**0.04**	**0.04**	**0.06**	**0.04**	**0.04**	-0.02	**0.03**	**0.02**
	Gilgit	**0.04**	**0.03**	**0.04**	**0.05**	**0.06**	-0.01	-0.01	-0.02	-0.01	0.02	**0.05**	**0.05**	**0.04**	**0.04**	-0.01	**0.02**	**0.02**
	Bunji	**0.02**	0.01	**0.04**	0.00	0.01	**-0.06**	**-0.05**	**-0.05**	**-0.04**	-0.04	**0.03**	0.02	**0.02**	0.02	**-0.05**	-0.02	0.00
	Chilas	-0.01	-0.01	0.03	0.01	0.02	**-0.05**	-0.02	-0.02	-0.02	0.00	0.00	0.01	0.00	0.02	**-0.03**	0.00	0.00
Tn	Skardu	0.00	0.02	0.00	-0.01	-0.01	**-0.04**	**-0.04**	**-0.04**	**-0.04**	**-0.05**	**-0.02**	0.01	0.01	0.00	**-0.04**	**-0.04**	**-0.02**
	Astore	0.02	0.01	**0.03**	**0.03**	**0.04**	0.00	-0.02	**-0.02**	-0.01	0.00	**0.02**	0.01	0.01	**0.04**	-0.01	0.01	**0.01**
	Gupis	**-0.04**	-0.02	-0.01	-0.03	-0.01	**-0.07**	**-0.06**	**-0.07**	**-0.05**	-0.03	**-0.03**	-0.01	**-0.03**	-0.02	**-0.07**	**-0.05**	**-0.04**
	Gilgit	0.00	**0.03**	0.00	-0.01	0.01	**-0.02**	**-0.05**	-0.03	-0.01	**-0.02**	-0.01	0.01	0.01	0.00	**-0.03**	**-0.02**	-0.01
	Bunji	0.01	0.01	0.03	0.00	0.00	-0.03	**-0.04**	-0.03	-0.03	-0.03	0.00	0.01	-0.01	0.01	**-0.04**	-0.04	0.00
	Chilas	**0.04**	0.02	0.01	0.01	0.03	-0.02	-0.01	**-0.03**	-0.02	0.00	**0.03**	**0.04**	**0.03**	0.02	**-0.02**	0.00	0.01
Tavg	Skardu	0.03	0.04	**0.03**	**0.02**	**0.03**	-0.01	-0.02	-0.02	-0.01	0.00	**0.02**	0.03	**0.03**	**0.03**	-0.02	0.00	0.01
	Astore	0.02	0.01	**0.04**	**0.04**	**0.05**	0.00	-0.01	**-0.02**	0.00	0.01	**0.03**	0.02	0.01	**0.05**	-0.01	**0.02**	**0.01**
	Gupis	0.00	0.00	0.00	0.01	0.03	**-0.04**	**-0.05**	**-0.05**	**-0.03**	0.00	0.01	0.02	0.00	0.01	**-0.04**	-0.01	-0.01
	Gilgit	**0.02**	**0.03**	0.02	0.02	**0.04**	-0.02	**-0.03**	**-0.03**	**-0.02**	-0.01	**0.03**	**0.03**	**0.03**	**0.02**	**-0.03**	0.00	0.00
	Bunji	0.00	0.01	0.02	-0.01	-0.01	**-0.04**	**-0.05**	**-0.04**	**-0.05**	**-0.04**	0.00	0.01	0.01	0.01	**-0.04**	**-0.03**	0.00
	Chilas	0.02	0.00	0.01	0.01	0.03	-0.03	-0.02	-0.02	-0.02	0.00	**0.02**	0.02	0.01	0.02	**-0.03**	0.00	0.00
DTR	Skardu	**0.06**	0.02	**0.05**	**0.07**	**0.09**	**0.05**	**0.06**	**0.03**	**0.06**	**0.09**	**0.09**	**0.05**	**0.05**	**0.07**	**0.05**	**0.09**	**0.06**
	Astore	**0.04**	0.00	0.01	0.02	0.02	**-0.02**	**0.01**	**0.02**	0.01	**0.02**	0.02	0.01	0.02	0.01	0.00	**0.02**	**0.02**
	Gupis	**0.08**	**0.06**	**0.05**	**0.07**	**0.09**	**0.06**	**0.06**	0.04	**0.07**	**0.10**	**0.09**	**0.08**	**0.09**	**0.06**	**0.05**	**0.08**	**0.07**
	Gilgit	0.04	0.02	**0.04**	**0.07**	**0.06**	0.00	**0.05**	**0.04**	**0.05**	**0.05**	**0.07**	**0.05**	**0.04**	**0.04**	**0.03**	**0.06**	**0.04**
	Bunji	**0.04**	0.01	**0.03**	0.01	0.03	0.00	0.00	-0.01	0.03	0.02	**0.06**	0.04	**0.04**	0.02	0.00	0.03	0.02
	Chilas	-0.04	-0.02	0.00	0.00	0.00	**-0.03**	-0.01	0.01	0.01	-0.01	-0.02	-0.03	-0.03	0.00	**-0.01**	-0.01	**-0.02**
P	Skardu	**0.30**	0.32	0.16	0.16	-0.02	0.08	0.06	**0.19**	0.07	0.00	0.00	0.15	**0.98**	0.45	**0.29**	0.12	**1.76**
	Astore	0.00	-0.28	**-0.78**	-0.51	-0.25	0.27	**0.19**	0.06	0.02	-0.05	0.02	-0.08	0.24	-1.31	0.45	0.06	-1.33
	Gupis	**0.08**	0.04	**0.28**	0.30	-0.08	0.00	**0.24**	0.18	0.00	0.00	0.00	0.00	0.11	0.20	0.32	-0.09	2.00
	Gilgit	0.00	0.00	-0.02	0.05	-0.05	**0.23**	0.01	0.01	0.03	0.00	0.00	0.00	0.02	-0.44	0.28	0.10	0.38
	Bunji	0.00	-0.06	-0.14	0.02	-0.17	0.09	0.05	0.12	0.11	-0.03	0.00	0.00	0.13	**-0.59**	0.36	0.09	0.21
	Chilas	0.00	0.03	-0.12	0.00	-0.01	**0.10**	0.07	0.07	**0.07**	-0.02	0.00	0.00	0.25	-0.12	**0.51**	0.03	0.70
Q	UIB-East	0.58	**0.89**	**1.18**	0.80	0.08	-12.94	**-21.37**	-10.53	-1.42	-0.18	0.06	0.16	0.55	1.10	**-14.86**	-0.57	-1.59
	Eastern-Kara.	0.00	0.00	-0.04	-0.08	**1.79**	**6.46**	5.17	6.81	4.34	**1.31**	**0.24**	0.00	0.07	0.41	**7.08**	**2.05**	**2.43**
	Central-Kara.	0.32	-0.07	-0.51	**-0.67**	**6.13**	3.85	-1.22	6.30	-7.40	**-4.08**	-1.36	-0.29	-0.35	1.75	6.22	-2.80	0.31
	Kachura	**1.04**	**1.40**	**1.19**	0.43	**6.06**	**12.88**	14.75	**19.45**	**14.27**	**3.69**	**1.14**	**1.13**	**1.12**	**2.67**	**19.20**	**6.12**	**7.19**
	UIB-Central	0.35	0.21	-0.19	-0.43	**9.99**	20.49	13.74	**20.73**	-4.95	-2.15	-0.80	-0.29	-0.30	**2.76**	17.69	-2.84	3.30
	Western-Kara.	0.04	0.00	0.00	0.00	0.29	**-3.75**	**-12.69**	**-13.75**	**-2.14**	-0.24	0.18	0.20	0.13	0.24	**-10.23**	-0.59	**-2.55**
	Karakoram	0.28	-0.20	-0.60	0.33	9.67	24.33	8.29	8.13	-7.57	-2.18	-0.59	0.63	-0.15	**4.17**	24.39	-4.36	6.44
	Hindukush	0.00	0.05	0.04	0.19	**3.31**	-1.00	-0.85	0.11	0.64	0.23	0.15	0.13	0.04	**1.25**	0.24	0.31	0.48
	UIB-WU	**0.58**	**0.60**	**0.33**	0.51	3.55	-1.86	**-12.74**	**-12.50**	0.68	1.48	**1.02**	**0.71**	**0.48**	1.30	**-6.83**	1.22	-0.95
	Astore	0.28	0.24	**0.32**	**0.97**	**3.52**	1.29	-0.62	0.54	0.16	0.28	0.32	0.23	0.31	**1.63**	0.43	0.28	**0.76**
	Partab_Bridge	**1.01**	0.49	0.44	**1.93**	**18.03**	13.07	12.89	-8.37	9.74	**3.84**	**2.61**	**1.63**	**1.74**	**6.84**	7.05	**4.93**	**4.72**
	UIB-WL	**1.94**	**1.96**	**3.49**	0.17	2.89	-12.90	-25.95	-12.06	-1.35	1.57	**1.94**	**2.35**	**1.92**	1.93	-13.82	0.48	-2.63
	UIB-WL-Partab	**1.58**	**1.87**	**2.11**	-0.82	-0.30	**-22.26**	-16.35	-17.07	0.02	-2.20	0.23	**1.18**	**1.32**	0.34	-22.10	-0.99	-5.40
	UIB_West	**2.02**	**2.01**	**2.73**	1.12	8.00	**-19.88**	**-32.88**	**-23.24**	-5.13	1.95	**2.59**	**2.40**	**2.18**	3.99	**-25.21**	0.93	-4.03
	Himalaya	**3.23**	**3.91**	**4.73**	2.33	-0.33	-32.29	**-69.33**	-17.55	-4.61	-0.05	**3.40**	2.05	**3.37**	6.86	-40.09	-0.72	-6.13
	UIB	**3.00**	**3.33**	**3.53**	0.62	**12.97**	-8.84	-13.31	-3.24	8.19	**4.03**	**3.92**	**3.04**	**3.04**	**5.00**	-6.15	**5.14**	2.23

911

Table 7. Field significant climatic trends for ten sub-regions along with their discharge (Q) trends at monthly to annual timescales over the period 1995-2012. Bold Q values indicate significant trends at 90% level.

Sub-regions	Vars.	Jan	Feb	Mar	Apr	May	Jun	Jul	Aug	Sep	Oct	Nov	Dec	DJF	MAM	JJA	SON	Ann.
Astore	Tx	-0.17									-0.21		-0.42	-0.16				-0.06
	Tn							-0.10			-0.10		-0.12				-0.10	
	Tavg	-0.15						-0.13			-0.21							-0.05
	DTR		-0.22							-0.13			-0.17	-0.07			-0.06	-0.08
	P			-3.73	-7.50	-4.60	-2.18	-1.90	-1.80	-2.11					-19.25	-6.02	-18.93	-38.01
	Q	0.05	0.00	0.22	0.50	7.65	4.26	-3.01	5.00	-1.00	-1.11	-0.67	0.00	0.00	2.20	1.97	-0.89	2.16
Hindukush	Tx		-0.11	0.23				-0.19		-0.29			-0.18				-0.12	-0.09
	Tn								0.25	0.24		-0.18	-0.24			0.09	0.10	
	Tavg			0.18				-0.11	0.08	-0.25			-0.13				-0.10	
	DTR	-0.21		-0.11	-0.18	-0.25	-0.28	-0.19	-0.36	-0.40	-0.52	-0.38		0.03	-0.16	-0.18	-0.33	-0.20
	P	1.30		-1.94				1.00		1.05	0.31		1.31	4.73	-10.19	-9.80	2.39	
	Q	0.87	0.26	0.15	1.27	2.05	3.49	-6.61	**14.02**	**7.03**	2.17	1.82	1.06	0.75	1.00	3.94	4.44	4.00
Himalaya	Tx	-0.17	-0.10					-0.22		-0.21	-0.19		-0.28	-0.16		-0.07	-0.12	-0.06
	Tn		-0.23	0.26			-0.14	-0.15	0.18		-0.16	-0.18	-0.14	-0.18		-0.13	-0.14	0.02
	Tavg	-0.15		0.25				-0.18	0.17	-0.18	-0.18	-0.09	-0.08	-0.11		-0.10	-0.13	-0.07
	DTR	-0.02	-0.20	0.18	-0.18			-0.13	-0.18	-0.36	-0.25			-0.12		-0.08	-0.19	-0.09
	P			-2.29	-5.71	-4.60	-2.18	-1.90	-1.80	-2.11			0.42		-12.15	-6.02	-18.93	-38.01
	Q	0.30	-0.32	4.10	0.91	43.99	62.23	12.43	83.33	22.43	9.97	2.32	0.23	1.17	26.64	**57.88**	7.75	**24.66**
West Karakoram	Tx			0.23				-0.18		-0.17	-0.16			-0.06				
	Tn		0.22	0.13				-0.13						0.17				0.05
	Tavg	-0.15		0.22	-0.09			-0.14		-0.15								
	DTR		-0.22							-0.13			-0.17	-0.07			-0.06	-0.08
	P					1.17	1.09						3.81	9.08				
	Q	1.20	1.00	1.50	**2.00**	0.59	12.09	-4.53	-4.09	**6.40**	**3.50**	**3.82**	**2.03**	**1.88**	1.00	-1.64	**5.43**	2.50
Karakoram	Tx		-0.11	0.23				-0.18		-0.22	-0.16			-0.06			-0.12	-0.06
	Tn		-0.11	0.23				-0.18		-0.22	-0.16			-0.06			-0.12	-0.06
	Tavg		0.22	0.13			-0.14	-0.14	0.25	0.46	-0.16	-0.18	-0.16	0.17		-0.08	0.06	-0.05
	DTR	-0.15		0.22	-0.09			-0.15	0.08	-0.16	-0.12	-0.09				-0.13	-0.14	-0.08
	P		2.95	1.97		1.17	1.72		1.58	2.15	1.43	2.40	2.69	6.39		5.39	5.76	45.07
	Q	1.88	2.00	1.33	1.00	-5.82	-7.80	**-64.97**	-37.17	-9.48	0.60	**8.97**	**5.97**	**1.65**	0.11	-24.43	5.64	-3.90
UIB Central	Tx							-0.26		-0.20	-0.16						-0.12	
	Tn			0.26			-0.14	-0.20			-0.16	-0.18	-0.16			-0.17	-0.18	0.02
	Tavg			0.25				-0.20		-0.18	-0.15	-0.09				-0.13	-0.14	-0.08
	DTR	0.13										0.09						
	P		2.95	1.97			2.35		1.58	2.15	1.43	2.40	1.57	5.99		5.39	5.76	45.07
	Q	**2.19**	1.81	2.02	-0.84	6.89	-18.08	**-43.79**	-20.20	-4.88	1.05	**4.38**	**2.34**	**2.00**	1.79	-18.34	2.01	-2.47
UIB	Tx	-0.14	-0.11	0.40				-0.20		-0.22	-0.20		-0.25			-0.09	-0.12	-0.09
	Tn		0.49	0.38				-0.13	0.31				-0.17			0.37	-0.14	0.27
	Tavg			0.37				-0.15	0.13	-0.18	-0.16		-0.11			-0.10	-0.12	-0.08
	DTR		-0.19		-0.14			-0.17	-0.24	-0.25	-0.38			0.11	-0.13	-0.10	-0.17	-0.09
	P			-2.17		1.17	-1.42		-2.40	1.65	1.10		1.97	5.98	-11.49	-7.91	3.68	
	Q	1.82	**5.09**	5.37	-2.50	11.35	14.67	-46.60	41.71	35.22	10.17	5.29	0.75	1.91	15.72	-1.40	19.35	4.25
UIB West	Tx	-0.14	-0.11	0.23				-0.18		-0.22	-0.21		-0.25	-0.11		-0.09	-0.12	-0.10
	Tn							-0.12	0.22				-0.18				-0.13	
	Tavg	-0.15		0.20				-0.13	0.13	-0.19	-0.19		-0.11				-0.11	-0.07
	DTR	-0.18	-0.20	-0.10	-0.16			-0.17	-0.24	-0.27	-0.38			-0.10	-0.13	-0.10	-0.19	-0.10
	P			-2.17	-5.71	1.17			-2.40	1.40			1.71	6.90	-11.49	-7.91	2.63	
	Q	2.45	1.37	5.43	2.42	**61.35**	54.89	0.21	42.93	**28.24**	**13.68**	**5.87**	1.38	2.00	**23.43**	44.18	**17.71**	**22.17**
UIB West Lower	Tx	-0.17	-0.10					-0.16		-0.21	-0.20		-0.28	-0.16		-0.07	-0.13	-0.06
	Tn		-0.23					-0.10	0.18				-0.12	-0.18		-0.08	-0.12	
	Tavg	-0.15						-0.13	0.17		-0.19		-0.07	-0.11		-0.06	-0.11	-0.07
	DTR	-0.15	-0.20	0.18	-0.18			-0.13	-0.18	-0.36	-0.25			-0.12		-0.08	-0.19	-0.09
	P			-2.29	-5.71	-4.60	-2.18	-1.90	-1.80	-2.11			0.42		-12.15	-6.02	-18.93	-38.01
	Q	1.88	0.41	6.39	-0.52	41.58	**59.50**	28.19	**81.58**	**30.99**	16.18	5.17	2.33	1.92	19.90	**65.53**	**16.02**	**25.44**
UIB West Upper	Tx	-0.14	-0.11	0.23				-0.18		-0.22	-0.21		-0.25	-0.11		-0.09	-0.12	-0.10
	Tn		0.22	0.13				-0.13	0.25	0.24		-0.18	-0.24	0.17		0.09	0.10	0.05
	Tavg	-0.15		0.20	-0.09			-0.13	0.08	-0.20			-0.13				-0.10	
	DTR	-0.21	-0.22	-0.11	-0.18	-0.25	-0.28	-0.19	-0.36	-0.28	-0.52	-0.38	-0.17	0.06	-0.16	-0.11	-0.19	-0.11
	P	1.30		-1.94		1.17	1.09	1.00		1.40	0.31		2.14	6.90	-10.19	-9.80	2.63	
	Q	1.24	**1.02**	1.39	**2.38**	**16.85**	12.38	-25.48	-15.50	-1.28	0.69	0.98	0.52	0.55	**7.76**	-3.68	0.45	-1.25

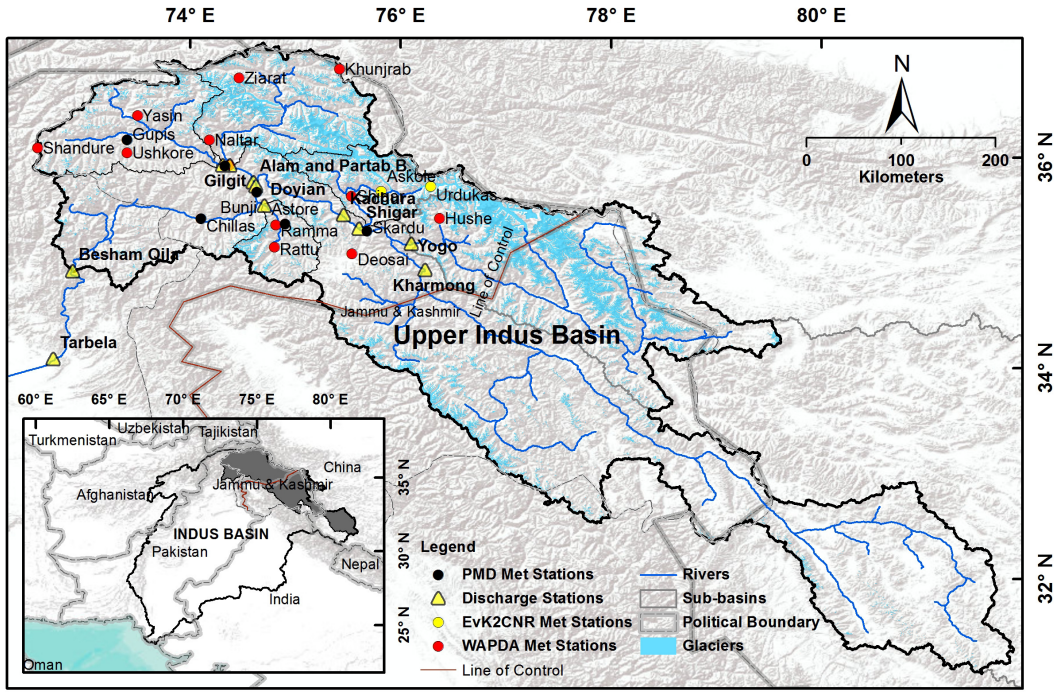

Figure 1: The upper Indus basin (UIB) and meteorological station networks

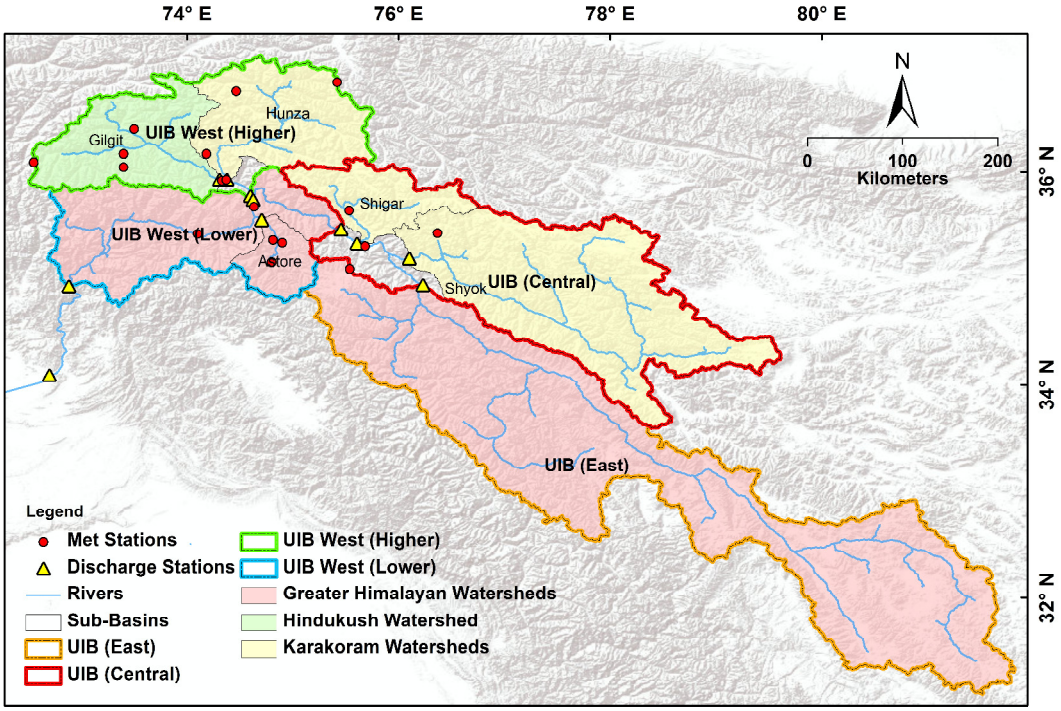

Figure 2: Hydometric stations and the sub-regions considered for field significance

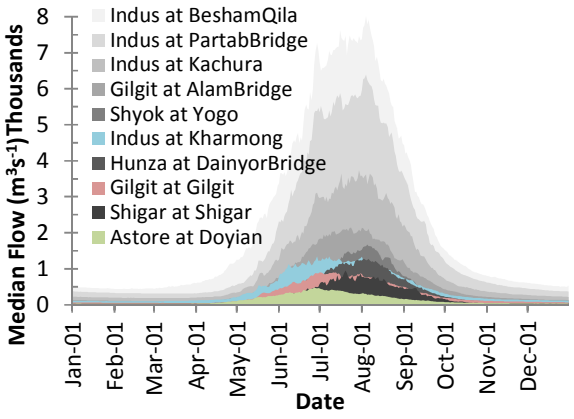

Figure 3: Long-term median hydrograph for ten gauges separating the sub-basins of the UIB featuring either mainly snow-fed (in color) or glacier-fed (in greyscale) hydrological regimes.

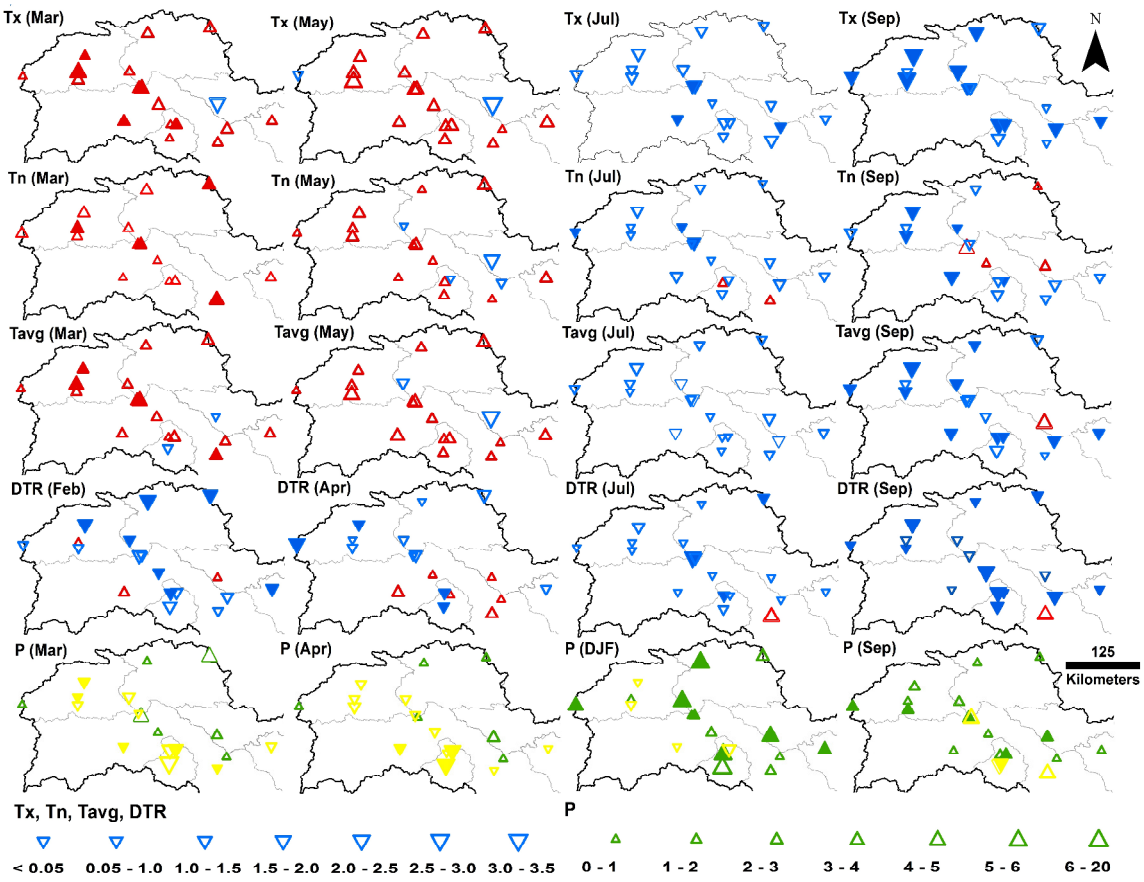

Figure 4: Trends per time step in Tx, Tn, Tavg, DTR (°C) and P (mm) for select months and seasons. Triangles pointing upward (downward) or in green/red (blue/yellow) colors show increasing (decreasing) trends. Solid (hollow) triangles indicate significant (insignificant) trends at 90% level.